

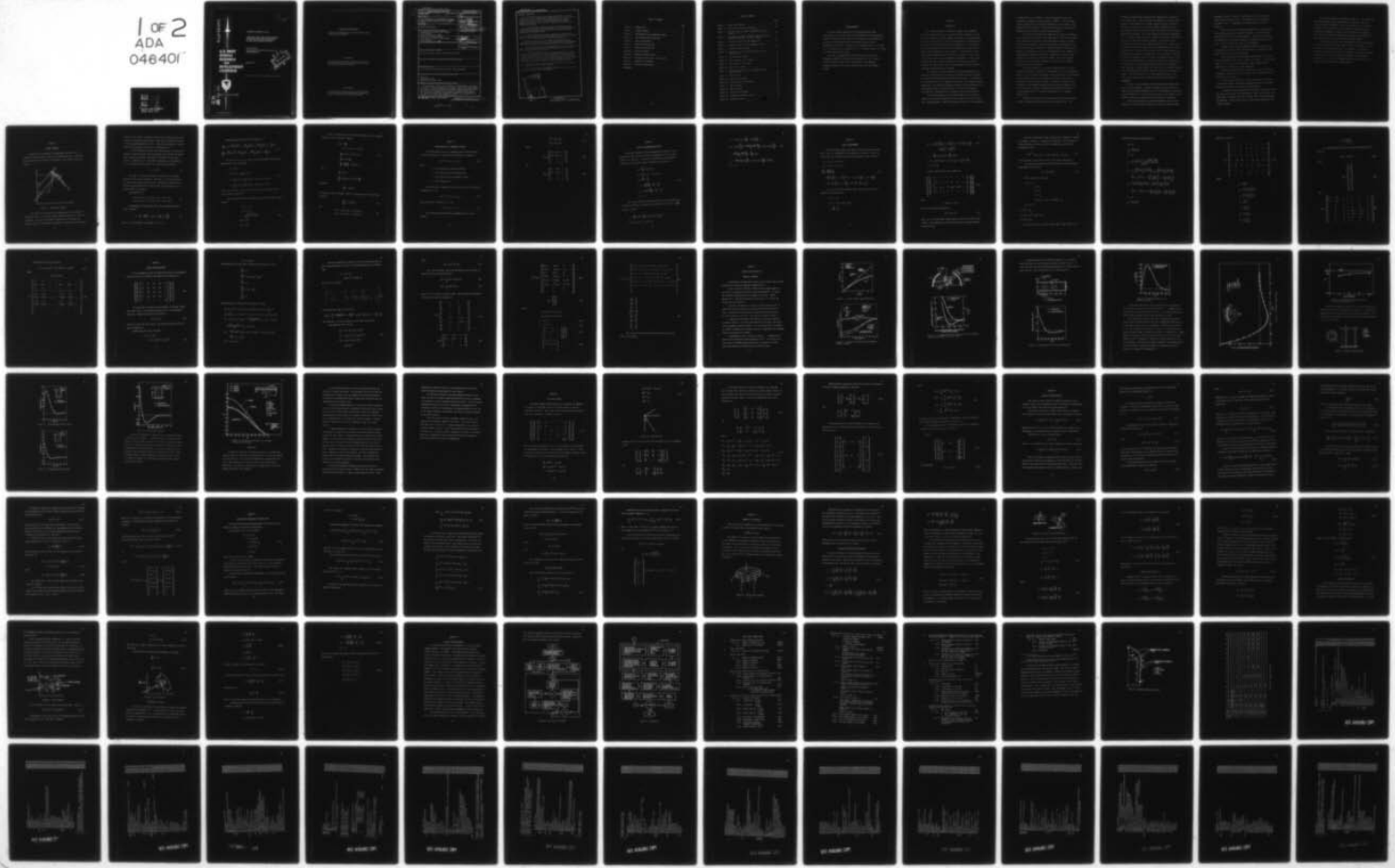
AD-A046 401 ARMY MISSILE RESEARCH AND DEVELOPMENT COMMAND REDSTO--ETC F/G 20/11
NONLINEAR ANALYSIS OF ORTHOTROPIC, LAMINATED SHELLS OF REVOLUTI--ETC(U)
AUG 77 C M ELDRIDGE

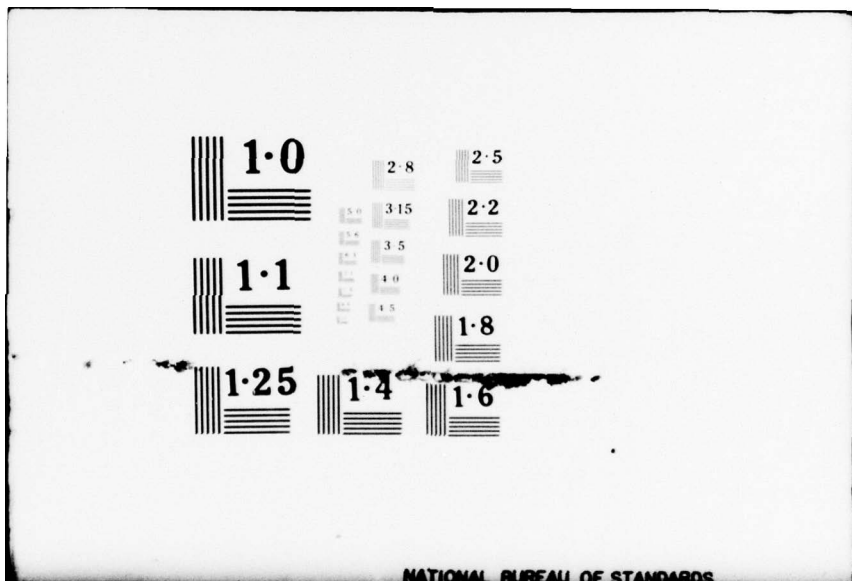
UNCLASSIFIED

DRDMI-TL-77-9

NL

1 of 2
ADA
046401





C. B. J.

AD A 046401



**U. S. ARMY
MISSILE
RESEARCH
AND
DEVELOPMENT
COMMAND**



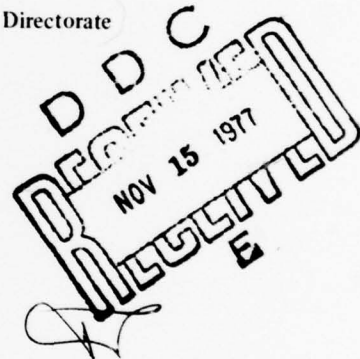
Redstone Arsenal, Alabama 35809

TECHNICAL REPORT TL-77-9

NONLINEAR ANALYSIS OF ORTHOTROPIC,
LAMINATED SHELLS OF REVOLUTION
BY THE FINITE ELEMENT METHOD

Charles M. Eldridge
Ground Equipment and Missile Structures Directorate
Technology Laboratory

August 1977



APPROVED FOR PUBLIC RELEASE: DISTRIBUTION UNLIMITED.

AD N.0.
DDC FILE COPY

DISPOSITION INSTRUCTIONS

**DESTROY THIS REPORT WHEN IT IS NO LONGER NEEDED. DO NOT
RETURN IT TO THE ORIGINATOR.**

DISCLAIMER

**THE FINDINGS IN THIS REPORT ARE NOT TO BE CONSTRUED AS AN
OFFICIAL DEPARTMENT OF THE ARMY POSITION UNLESS SO DESIG-
NATED BY OTHER AUTHORIZED DOCUMENTS.**

TRADE NAMES

**USE OF TRADE NAMES OR MANUFACTURERS IN THIS REPORT DOES
NOT CONSTITUTE AN OFFICIAL INDORSEMENT OR APPROVAL OF
THE USE OF SUCH COMMERCIAL HARDWARE OR SOFTWARE.**

UNCLASSIFIED

SECURITY CLASSIFICATION OF THIS PAGE (When Data Entered)

REPORT DOCUMENTATION PAGE		READ INSTRUCTIONS BEFORE COMPLETING FORM
1. REPORT NUMBER TL-77-9	2. GOVT ACCESSION NO.	3. RECIPIENT'S CATALOG NUMBER 9
4. TITLE (and Subtitle) NONLINEAR ANALYSIS OF ORTHOTROPIC, LAMINATED SHELLS OF REVOLUTION BY THE FINITE ELEMENT METHOD.		5. TYPE OF REPORT & PERIOD COVERED Technical Report
6. AUTHOR(s) Charles M. Eldridge		7. PERFORMING ORG. REPORT NUMBER TL-77-9
8. CONTRACT OR GRANT NUMBER(S) DA Proj No. 1L362303A214 AMCMS Code no. 63203.2140911.08		9. PROGRAM ELEMENT, PROJECT, TASK AREA & WORK UNIT NUMBERS
10. CONTROLLING OFFICE NAME AND ADDRESS Commander, US Army Missile R&D Command ATTN: DRDMI-TL Redstone Arsenal, AL 35809		11. REPORT DATE Aug 1977
12. NUMBER OF PAGES 103		13. SECURITY CLASS. (of this report) Unclassified
14. MONITORING AGENCY NAME & ADDRESS (if different from Controlling Office)		15. DECLASSIFICATION/DOWNGRADING SCHEDULE
16. DISTRIBUTION STATEMENT (of this Report) Approved for public release; distribution unlimited.		
17. DISTRIBUTION STATEMENT (of the abstract entered in Block 20, if different from Report)		
18. SUPPLEMENTARY NOTES This report was prepared from the author's Phd dissertation.		
19. KEY WORDS (Continue on reverse side if necessary and identify by block number) Structures Composite material Orthotropic, laminated shell		
20. ABSTRACT (Continue on reverse side if necessary and identify by block number) The nonlinear analysis of an orthotropic, laminated shell of revolution with transverse shear deformations is presented. The finite element method employing a curved shell element was the method used to perform the analysis. Each element has two nodes with four degrees of freedom at each node, viz., two translation, one bending rotation and one transverse shear rotation. The classical Kirchhoff-Love assumption for normals to the midsurface was relaxed in favor of the shear deformation mode.		

DD FORM 1 JAN 73 1473 EDITION OF 1 NOV 65 IS OBSOLETE

UNCLASSIFIED
SECURITY CLASSIFICATION OF THIS PAGE (When Data Entered)

410263

Done

UNCLASSIFIED

SECURITY CLASSIFICATION OF THIS PAGE(When Data Entered)

Abstract - Continued

A curved shell element was developed that matches slopes and curvatures as well as displacements at the nodal circles. This significantly reduces the meridional bending moments present at element junctures as compared to the case in which straight line elements (conical frusta) are used to represent a shell of revolution having meridional curvatures.

A local rectilinear coordinate system was established for the element to represent the displacement patterns. The displacements of the curved element were represented in this local system and subsequently transferred to the global system.

A computer program was written in Fortran IV to implement the theory. Several example problems, both linear and nonlinear, were solved and the results compared with solutions from the literature.

The program can be used for analysis of orthotropic shells including fiber composite structures. The angle of wrap and longitudinal and transverse material physical properties are part of the input data.

Two point Gaussian Quadrature Integration was used in the development of the stiffness matrix. The shell thickness and pressure load may vary linearly along the meridian.

An incremental method was used for obtaining the nonlinear effects. The load can be applied in increments. From the first load increment, a linear solution is obtained. The coordinates are then updated and a second solution is found using the second load increment. This procedure is continued until the total load is reached. Excellent agreement with both linear and nonlinear problems from the literature was obtained.

The program requires relatively short execution time and can be run interactively on the CDC 6600 computer.

Some areas of further investigation which are logical and useful extensions of this work were recommended.



UNCLASSIFIED

SECURITY CLASSIFICATION OF THIS PAGE(When Data Entered)

TABLE OF CONTENTS

	Page
Chapter 1. INTRODUCTION	1
Chapter 2. ELEMENT GEOMETRY	6
Chapter 3. TRANSFORMATION OF COORDINATE SYSTEMS	10
Chapter 4. STRAIN-DISPLACEMENT RELATIONS.	12
Chapter 5. SHELL DISPLACEMENTS.	14
Chapter 6. STRESS-STRAIN RELATIONS.	21
Chapter 7. RESULTS AND CONCLUSIONS	27
Appendix A. ELASTICITY MATRIX.	39
Appendix B. ELEMENT STIFFNESS MATRIX	44
Appendix C. EQUILIBRIUM EQUATIONS BY VIRTUAL WORK.	50
Appendix D. THEORETICAL BACKGROUND	55
Appendix E. COMPUTER PROGRAM ORTHO2.	66
REFERENCES.	101

LIST OF FIGURES

	Page
Figure 1. Curved Shell Element	6
Figure 2. Circular Plate, Large Deflections.	28
Figure 3. Circular Flat Plate Under Axisymmetric Pressure Loading.	28
Figure 4. A Hemispherical Shell Solution by Finite Elements (Grafton and Strome, J.A.I.A.A., 1963)	29
Figure 5. Cylindrical Shell With Unit Edge Load	30
Figure 6. Meridional Moment for the Cylindrical Shell.	31
Figure 7. Meridional Bending Moment.	32
Figure 8. Convergence of Center Deflection of Circular Sandwich Plate	33
Figure 9. Locally Loaded Cylinder.	33
Figure 10. Bending Moment Versus Length	34
Figure 11. Displacement Versus Length	34
Figure 12. Shear Versus Length.	35
Figure 13. Transverse Deflections in a Clamped Circular Sandwich Plate	36
Figure 14. Material Axes.	40
Figure 15. Typical Shell Element.	55
Figure 16. Transverse Shear Deformation	58
Figure 17. Shell Geometry	62
Figure 18. Shell Meridian	63
Figure 19. Flow Chart for ORTHO2.	67
Figure 20. Hemisphere-Cylindrical Shell	73
Figure 21. Sample Data Cards.	74

ACKNOWLEDGMENTS

The author hereby expresses his sincere gratitude and deep appreciation to Dr. Ju-chin Huang of the Engineering Science Department, Tennessee Technological University for his guidance, encouragement, and constant surveillance during the formulation of the theory and development of this work. Gratitude is also extended to Dr. D. G. Smith, Dr. S. B. Khleif, Dr. G. R. Buchanan, Dr. D. H. Deason, and Mr. D. K. Buck for their advice and assistance.

Gratitude is expressed to the US Army Missile Research and Development Command for providing the opportunity for this research. A special thanks is given to Mr. John Sofferis of the Command's Computation Center for his advice and assistance with the computer program.

Chapter 1

INTRODUCTION

The continuing search for lighter, stronger, more economical structures, particularly in the aircraft and missile industry, has led to the investigation of various composite materials as a possible applicable type of construction. Many of these materials are orthotropic and multi-layered and have nonlinear physical properties. Tests on actual structures have proven that some of these materials are unlike conventional structural materials in many respects. Although much has been learned about composite material behavior in the past few years, there are still many areas that are unknown and unpredictable. These characteristics pose many difficult problems for the designer and analyst. To obtain the most efficient use of these composites, suitable analysis and design techniques must be developed.

The aircraft and missile industries have many applications for shells of revolution and are continually searching for ways to decrease the weight while maintaining or increasing the strength. The possibility of achieving this by use of composites has created much interest in their application. The need for techniques to analyze these structures was the prime motivation for this present effort. This study investigates an orthotropic, laminated shell of revolution with shear deformation.

The rapid development of the digital computer in the last two decades has contributed significantly to the analyst's ability to treat these complex problems. Numerical methods that would have been impossible

to employ prior to the computer are now quite popular and are used extensively throughout the stress analysis community. Both the finite element method and finite difference techniques are used today to solve complex structural problems. Each of these has features which make its application more suitable to a particular type problem.

The finite element method was chosen for this present development for several reasons. Because of the flexibility of their size and shape, finite elements can represent a given body, however complex its shape may be, quite accurately. Structures with holes or discontinuities can be treated with little difficulty. Problems involving variable material properties and geometry such as are encountered with fiber composites do not present any additional difficulty. Geometrical and material non-linearity can be dealt with relatively easily. One of the principal assets of the finite element method is the ease with which boundary conditions can be represented.

The essential feature of the finite element method is that the governing differential equations of equilibrium of the shell are approximated by a set of algebraic equations. This is equivalent to substituting, for the actual structure, an assemblage of discrete elements interconnected at a finite number of nodes. The element stiffness is then evaluated and superimposed to obtain the total stiffness matrix of the entire structure. Finally, the nodal force equilibrium equations are solved simultaneously for the nodal displacements of the complete system [1-5].

In shells of revolution, the structure is divided into a number of short frustums which are connected at their nodal circle. The

assemblage is made through equilibrium and compatibility requirements at the nodal circle. Mayer and Harmon [6] employed the conical frustum (singly curved) element in the earlier stage of analysis of shells of revolution. Popov et al. [7] used the bending displacements due to edge loadings from the exact shell theory rather than the usual assumed displacement functions. Their result showed no significant improvement over the simpler assumed functions. Grafton and Strome [8] used conical elements in a true finite element technique. The results are very satisfactory for shells with a straight generated curve. However, there are still some inaccurate moments due to the approximation of a doubly curved shell by a singly curved element. This is mainly caused by the discontinuity of slope at the nodal circle of the substitute structure. To remedy this problem, Jones and Strome [9] developed a doubly curved element which matched both the location and slope of the original shell at nodal circles, thus avoiding unwanted discontinuities of slope at these locations. Khojasteh-Bakht [10] used two local coordinate systems, viz., curvilinear and rectilinear coordinate systems, to formulate his element. The latter proved to be a better approach because it can treat certain constant strain states which the former was unable to accommodate.

Recently, a finite-element technique including transverse shear effect has been attempted. Clough and Felippa [11] have described a simple shear distortion mechanism which can be implemented by expressing the total rotation of a cross section as the sum of the rotation on the middle surface plus a uniform shear strain through the thickness.

Klein [12] has applied the matrix displacement finite element approach to the linear elastic analysis of shells of revolution under

axisymmetric loads. The shell is idealized as a series of conical frusta, joined at nodal circles. The external forces are applied at the nodal circles. A comparison with these solutions is made in Chapter 7.

Sharifi [13] used an incremental formulation for the nonlinear finite element analysis of sandwich structures. The nonlinearities considered were due to large displacements. Included in the analysis are axisymmetric shells with axisymmetric loadings and boundary conditions. Curved elements were used in the development.

McNamara [14] investigated nonlinear dynamic problems by using an incremental stiffness finite element analysis. Both geometric and material nonlinearities were considered.

Becker and Brisbane [15] developed the equations for an axisymmetric, orthotropic shell using a straight line element. Their development did not include shear deformations. Shear deformations are important for the analysis of fiber composites.

Nickell and Sato [16] used a curved shell element to analyze an orthotropic, layered shell of revolution. Shear deformations were not included in their analysis.

In this present effort, the finite element method is used with a curved shell element considering a nonlinear laminated, orthotropic shell of revolution and transverse shear deformations.

A polynomial representation of the meridional curve of the shell was chosen which matches the displacements, slope, and curvature at the nodal points. Nonlinear terms are included in the strain-displacement relationships. The stiffness matrix is then derived using these nonlinear relations.

There are four degrees of freedom at a node, viz., two translation, one bending rotation and one transverse shear rotation. The field equations similar to Reissner's theory of thick plates [5] were used as a guideline for formulating the shear deformation degree of freedom. The procedure employed was similar to that of Clough and Felippa [11]. The classical Kirchhoff-Love assumption for normals to the midsurface was relaxed in favor of the assumed shear deformation mode.

A computer program was written implementing the derived equations. The element stiffness matrix was formed by numerical integration. Much of the data is generated internally in the program. The program is limited to ten different materials and 50 nodes, but it can be increased by increasing the dimension statement accordingly. The program is relatively fast. Most of the example problems run required from 3 to 4 seconds execution time on the CDC 6600 computer.

Chapter 2

ELEMENT GEOMETRY

The shell to be considered is axisymmetric; therefore, it is sufficient to define only the shape of its meridional curve. The finite element method will be used for this analysis. The element is shown in Figure 1.

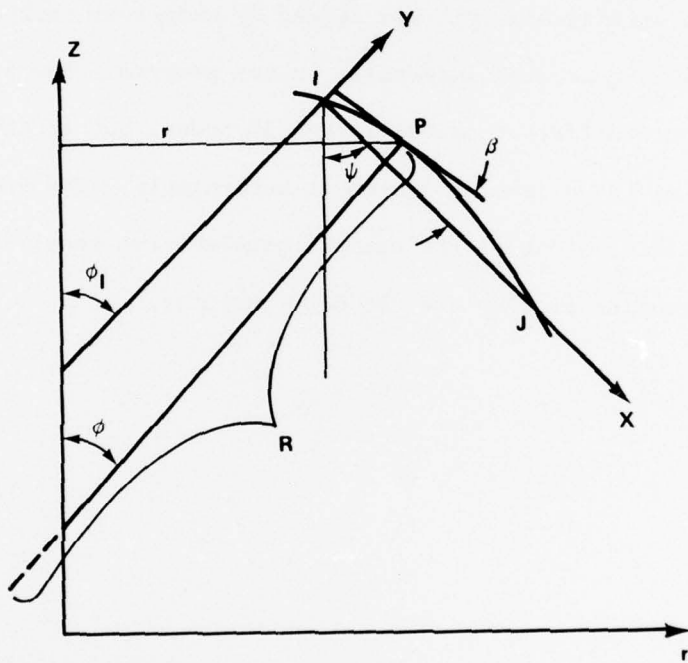


Figure 1. Curved Shell Element.

The element is curved and the two end points of the element are denoted by I and J. For a shell whose reference surface is a surface of revolution, the lines of principal curvature are its meridians and parallel circles. The principal curvilinear coordinates of the reference

surface are the angle ϕ between the normal to the reference surface and the axis of revolution and the angle θ describing the position of points on the corresponding parallel circle. Since this development is axisymmetric both in geometry and load, it is independent of θ .

A local coordinate system for each curved element is constructed between two adjacent nodal circles by drawing chords between the points. This rectangular Cartesian system which is normalized by the chord length ℓ is denoted by x-y. The global coordinates are represented by r-z. The angles shown in Figure 1 are related by the relation

$$\phi + \psi + \beta = \frac{\pi}{2} . \quad (1)$$

The angle ϕ is the angle between the normal to the reference surface and the axis of revolution. The angle ψ is the angle between the chord of the element and the z-axis. The angle β is defined to be the angle between the chord line (the x-axis) and the tangent to the curved surface at any point.

From Equation (1),

$$\begin{aligned} \sin \beta &= \cos (\phi + \psi) = \cos \phi \cos \psi - \sin \phi \sin \psi \\ \cos \beta &= \sin (\phi + \psi) = \sin \phi \cos \psi + \cos \phi \sin \psi . \end{aligned} \quad (2)$$

To approximate the meridional curve, the following substitute curve is assumed:

$$y = x \left(1 - \frac{x}{\ell} \right) \left(a_1 + a_2 \frac{x}{\ell} + a_3 \frac{x^2}{\ell^2} + a_4 \frac{x^3}{\ell^3} \right) \quad (3)$$

where ℓ = chord length of the element. ($0 < x < \ell$)

Differentiating Equation (3) with respect to x

$$\begin{aligned}\frac{dy}{dx} &= a_1 + \frac{2(a_2 - a_1)}{\ell} x + \frac{3(a_3 - a_2)}{\ell^2} x^2 + \frac{4(a_4 - a_3)}{\ell^3} x^3 - \frac{5a_4}{\ell^4} x^4 \\ \frac{d^2y}{dx^2} &= \frac{2(a_2 - a_1)}{\ell} + \frac{6(a_3 - a_2)}{\ell^2} x + \frac{12(a_4 - a_3)}{\ell^3} x^2 - \frac{20a_4}{\ell^4} x^3 .\end{aligned}\quad (4)$$

The constants a_1 , a_2 , a_3 , and a_4 can be determined by evaluating Equations (4) at the end points

$$\begin{aligned}a_1 &= \tan \beta_1 \\ a_2 &= \tan \beta_1 - \frac{\ell}{2R_1} \sec^3 \beta_1 \\ a_3 &= \frac{-\ell}{2R_2} \sec^3 \beta_2 + \frac{\ell}{R_1} \sec^3 \beta_1 - 4 \tan \beta_2 - 5 \tan \beta_1 \\ a_4 &= \frac{\ell}{2R_2} \sec^3 \beta_2 - \frac{\ell}{2R_1} \sec^3 \beta_1 + 3(\tan \beta_1 + \tan \beta_2) .\end{aligned}\quad (5)$$

where the subscripts 1 and 2 on β and R reference these items to the I and J nodes respectively.

The following geometrical relations are given with respect to the element:

$$\begin{aligned}\Delta r &= r_2 - r_1 \\ \Delta z &= z_1 - z_2 \\ \ell &= \sqrt{(\Delta r)^2 + (\Delta z)^2} \\ \sin \psi &= \frac{\Delta r}{\ell} \\ \cos \psi &= \frac{\Delta z}{\ell} .\end{aligned}\quad (6)$$

After the substitute curve has been established, all the geometric quantities can be written as follows:

$$\tan \beta = \frac{dy}{dx}$$

$$r = r_1 + x \sin \psi + y \cos \psi$$

$$\frac{dr}{dx} = \sin \psi + \tan \beta \cos \psi \quad (7)$$

$$\frac{d}{ds} = \cos \beta \frac{d}{dx}$$

$$\frac{d\beta}{dx} = \frac{d\beta}{ds} \frac{ds}{dx} = -\frac{1}{R} \sec \beta \quad .$$

Since

$$\frac{dy}{dx} = \tan \beta$$

$$\frac{d^2y}{dx^2} = \frac{d}{dx} (\tan \beta) = \sec^2 \beta \frac{d\beta}{dx} \quad ,$$

therefore

$$\frac{d\beta}{dx} = -\frac{1}{R} \sec \beta \quad .$$

The quantity $d\beta/ds$ is negative since β is decreasing as S is increasing.

Therefore

$$\frac{d^2y}{dx^2} = -\frac{1}{R} \sec^3 \beta \quad (8)$$

and

$$\begin{aligned} \cos \phi &= \sin \beta \cos \psi + \cos \beta \sin \psi \\ \sin \phi &= \cos \beta \cos \psi - \sin \beta \sin \psi \quad . \end{aligned} \quad (9)$$

Chapter 3

TRANSFORMATION OF COORDINATE SYSTEMS

The displacement vector of a material point on the midsurface in the local principal curvilinear shell coordinate is denoted by

$$\{f_c\}^T = [u_c, w_c, \chi_c, \gamma_c] \quad (10)$$

where

u_c = the displacement along the meridian.

w_c = the transverse (normal) displacement.

χ_c = the rotation about a meridional tangent.

γ_c = shear deformation.

The displacement components which refer to the local rectilinear coordinates, x-y, are

$$\{f_r\}^T = [u_r, w_r, \chi_r, \gamma_r] \quad (11)$$

and to the global coordinates, r-z, are

$$\{f\}^T = [u, w, \chi, \gamma] . \quad (12)$$

The transformation between these components can be seen as follows:

$$\begin{aligned}\{f_c\} &= [q_c] \{f_r\} \\ \{f_r\} &= [q_r] \{f\}\end{aligned}\tag{13}$$

where

$$[q_c] = \begin{bmatrix} \cos \beta & \sin \beta & 0 & 0 \\ -\sin \beta & \cos \beta & 0 & 0 \\ 0 & 0 & 1 & 0 \\ 0 & 0 & 0 & 1 \end{bmatrix} \tag{14}$$

and

$$[q_r] = \begin{bmatrix} \sin \psi & -\cos \psi & 0 & 0 \\ \cos \psi & \sin \psi & 0 & 0 \\ 0 & 0 & 1 & 0 \\ 0 & 0 & 0 & 1 \end{bmatrix} . \tag{15}$$

Chapter 4

STRAIN-DISPLACEMENT RELATIONS

The general nonlinear strain-displacement relations for large rotation but small strain were derived by Novozhilov [18] and later corrected by Tsao [19]. For shells of revolution with axisymmetric loading, the strain displacement relations can be written as

$$\begin{aligned}
 e_1 &= \frac{du_c}{ds} + \frac{w_c}{R} + \frac{1}{2} \chi_c^2 \\
 e_2 &= \frac{1}{r} (u_c \cos \phi + w_c \sin \phi) \\
 \chi_c &= \frac{dw_c}{ds} - \frac{u_c}{R} \\
 \kappa_1 &= -\frac{d}{ds} \left(\frac{dw_c}{ds} - \frac{u_c}{R} + \gamma_1 \right) \\
 \kappa_2 &= -\frac{\cos \phi}{r} \left(\frac{dw_c}{ds} - \frac{u_c}{R} + \gamma_1 \right) \\
 \gamma_1 &= -\gamma_c
 \end{aligned} \tag{16}$$

The strains defined in Equations (16) are now transformed into the local rectilinear coordinates as follows (recall that $ds = \frac{dx}{\cos \beta}$ and $\beta = \beta_1 - \frac{s}{R}$):

$$\begin{aligned}
 e_1 &= \frac{du_r}{dx} \cos^2 \beta + \frac{dw_r}{dx} \cos \beta \sin \beta + \frac{1}{2} (\chi_c)^2 \\
 e_2 &= \frac{1}{r} (u_r \sin \psi + w_r \cos \psi)
 \end{aligned}$$

$$\begin{aligned}
 \chi_c &= -\sin \beta \cos \beta \frac{du}{dx} + \cos^2 \beta \frac{dw}{dx} + \gamma_r \\
 \kappa_1 &= -\cos^3 \beta \frac{d^2 w}{dx^2} - \frac{2 \cos \beta \sin \beta}{R_1} \frac{dw}{dx} + \sin \beta \cos^2 \beta \frac{d^2 u}{dx^2} \quad (17) \\
 &\quad + \frac{\sin^2 \beta - \cos^2 \beta}{R_1} \frac{du}{dx} - \frac{dy}{dx} \cos \beta \\
 \kappa_2 &= -\frac{\cos \phi}{r} \left(\cos^2 \beta \frac{dw}{dx} - \sin \beta \cos \beta \frac{du}{dx} \right) - \frac{\cos \phi}{r} \gamma_r \\
 \gamma_1 &= -\gamma_r .
 \end{aligned}$$

Chapter 5

SHELL DISPLACEMENTS

The shell displacements are written in local rectilinear coordinates. They are represented by four degrees of freedom at a node: two translations, one bending rotation and one transverse shear rotation.

$$u_c = u_r \cos \beta + w_r \sin \beta$$

$$w_c = -u_r \sin \beta + w_r \cos \beta$$

$$\frac{dw_c}{ds} = \left(\frac{dw_c}{dx} \right) \frac{dx}{ds} \quad (18)$$

$$\begin{aligned} &= \frac{dx}{ds} \left(-\frac{du_r}{dx} \sin \beta + \frac{dw_r}{dx} \cos \beta - u_r \cos \beta \frac{d\beta}{dx} - w_r \sin \beta \frac{d\beta}{dx} \right) \\ &= \cos \beta \left(-\frac{du_r}{dx} \sin \beta + \frac{dw_r}{dx} \cos \beta + \frac{u_r}{r} + \frac{w_r}{r} \tan \beta \right) . \end{aligned}$$

As was done by Khojasteh-Bakht [10], the displacement field is assumed to be represented by

$$u_r = \alpha_1 + \alpha_2 x$$

$$w_r = \alpha_3 + \alpha_4 x + \alpha_5 x^2 + \alpha_6 x^3$$

$$\times_r = \frac{dw_c}{ds} - \frac{u_c}{r}$$

$$\begin{aligned}
 x_r &= \cos \beta \left(-\frac{du}{dx} \sin \beta + \frac{dw}{dx} \cos \beta + \frac{u}{r} + \frac{w}{r} \tan \beta \right) \\
 &\quad - \frac{u_r \cos \beta}{r} - \frac{w_r \sin \beta}{r} \\
 x_r &= -\frac{du}{dx} \sin \beta \cos \beta + \frac{dw}{dx} \cos^2 \beta + \gamma \\
 x_r &= -\alpha_2 \sin \beta \cos \beta + (\alpha_4 + 2 \alpha_5 x + 3 \alpha_6 x^2) \cos^2 \beta \\
 \gamma_r &= \alpha_7 + \alpha_8 x
 \end{aligned} \tag{19}$$

In matrix notation this can be written as:

$$\begin{Bmatrix} u_r \\ w_r \\ x_r \\ \gamma_r \end{Bmatrix} = \begin{bmatrix} 1 & x & 0 & 0 & 0 & 0 & 0 & 0 \\ 0 & 0 & 1 & x & x^2 & x^3 & 0 & 0 \\ 0 & -sc & 0 & c^2 & 2xc^2 & 3x^2c^2 & 0 & 0 \\ 0 & 0 & 0 & 0 & 0 & 0 & 1 & x \end{bmatrix} \begin{Bmatrix} \alpha_1 \\ \alpha_2 \\ \alpha_3 \\ \alpha_4 \\ \alpha_5 \\ \alpha_6 \\ \alpha_7 \\ \alpha_8 \end{Bmatrix} \tag{20}$$

where

$$s = \sin \beta, c = \cos \beta.$$

This can be written symbolically as

$$\{f_r\} = [\phi] \{\omega\} \tag{21}$$

where $\{\omega\}$ is the generalized displacements vector for the curved shell element. This displacement function allows rigid body motion without inducing strains.

The shell displacements shown in Equation (20) represent 4 degrees of freedom at a node, two translation, two rotation. The 8 degrees of freedom connected with the nodes of the element are written as the displacement vector

$$\{\delta_r^e\}^T = [u_{r1}, w_{r1}, x_{r1}, \gamma_{r1}, u_{r2}, w_{r2}, x_{r2}, \gamma_{r2}] . \quad (22)$$

where subscripts 1 and 2 refer to the I and J nodes respectively.

The generalized displacements $\{\alpha\}$ are related to the nodal point displacement vector $\{\delta_r^e\}$ by

$$\{\alpha\} = [A_r] \{\delta_r^e\} . \quad (23)$$

$\{\alpha\}$ is evaluated as follows:

1) At $x = 0$

$$\alpha_1 = u_{r1}$$

$$\alpha_3 = w_{r1}$$

$$\alpha_7 = \gamma_{r1}$$

$$-\alpha_2 \sin \beta_1 \cos \beta_1 + \alpha_4 \cos^2 \beta_1 = x_{r1} .$$

2) At $x = \ell$

$$\alpha_1 + \alpha_2 \ell = u_{r2}$$

$$\alpha_3 + \alpha_4 \ell + \alpha_5 \ell^2 + \alpha_6 \ell^3 = w_{r2}$$

$$\alpha_7 + \alpha_8 \ell = \gamma_{r2}$$

$$-\alpha_2 \sin \beta_2 \cos \beta_2 + \alpha_4 \cos^2 \beta_2 + 2\alpha_5 \ell \cos^2 \beta_2 + 3\alpha_6 \ell^2 \cos^2 \beta_2 = x_{r2} .$$

Solving this system of equations gives

$$\alpha_1 = u_{r1}$$

$$\alpha_2 = \frac{u_{r2} - u_{r1}}{\ell}$$

$$\alpha_3 = w_{r1}$$

$$\alpha_4 = \frac{x_{r1} + \sin \beta_1 \cos \beta_1 \left(\frac{u_{r2} - u_{r1}}{\ell} \right)}{\cos^2 \beta_1}$$

$$\alpha_5 = u_{r1} \left(\frac{\tan \beta_2 + 2 \tan \beta_1}{\ell^2} \right) - u_{r2} \left(\frac{\tan \beta_2 + 2 \tan \beta_1}{\ell^2} \right) \\ - \frac{3}{\ell^2} w_{r1} + \frac{3}{\ell^2} w_{r2} - x_{r1} \left(\frac{2}{\ell \cos^2 \beta_1} \right) - x_{r2} \left(\frac{1}{\ell \cos^2 \beta_2} \right)$$

$$\alpha_6 = - \frac{u_{r1} (\tan \beta_2 + \tan \beta_1)}{\ell^3} + \frac{u_{r2} (\tan \beta_2 + \tan \beta_1)}{\ell^3}$$

$$+ \frac{2}{\ell^3} w_{r1} - \frac{2}{\ell^3} w_{r2} + x_{r1} \left(\frac{1}{\ell^2 \cos^2 \beta_1} \right) + x_{r2} \left(\frac{1}{\ell^2 \cos^2 \beta_2} \right)$$

$$\alpha_7 = \gamma_{r1}$$

$$\alpha_8 = \frac{\gamma_{r2} - \gamma_{r1}}{\ell}$$

Therefore, from (23)

$$[A_r] = \begin{bmatrix} 1 & 0 & 0 & 0 & 0 & 0 & 0 & 0 \\ -\frac{1}{\ell} & 0 & 0 & 0 & \frac{1}{\ell} & 0 & 0 & 0 \\ 0 & 1 & 0 & 0 & 0 & 0 & 0 & 0 \\ -a_1 & 0 & b_1 & 0 & a_1 & 0 & 0 & 0 \\ a_2 & -\frac{3}{\ell^2} & -2b_2 & 0 & -a_2 & \frac{3}{\ell^2} & -b_4 & 0 \\ -a_3 & \frac{2}{\ell^3} & b_3 & 0 & a_3 & -\frac{2}{\ell^3} & b_5 & 0 \\ 0 & 0 & 0 & 1 & 0 & 0 & 0 & 0 \\ 0 & 0 & 0 & -\frac{1}{\ell} & 0 & 0 & 0 & \frac{1}{\ell} \end{bmatrix} \quad (24)$$

where

$$a_1 = \frac{\tan \beta_1}{\ell}$$

$$a_2 = \frac{2 \tan \beta_1 + \tan \beta_2}{\ell^2}$$

$$a_3 = \frac{\tan \beta_1 + \tan \beta_2}{\ell^3}$$

$$b_1 = \frac{1}{\cos^2 \beta_1}$$

$$b_2 = \frac{1}{\ell \cos^2 \beta_1}$$

$$b_3 = \frac{1}{\ell^2 \cos^2 \beta_1}$$

$$b_4 = \frac{1}{\ell \cos^2 \beta_2}$$

$$b_5 = \frac{1}{\ell^2 \cos^2 \beta_2} .$$

The transformation of $\{\delta_r\}^e$ to the global coordinate $\{\delta\}^e$ is given by

$$\{\delta_r\}^e = [R] \{\delta\}^e \quad (25a)$$

where

$$\{\delta\}^e = \begin{Bmatrix} u_1 \\ w_1 \\ x_1 \\ \gamma_1 \\ u_2 \\ w_2 \\ x_2 \\ \gamma_2 \end{Bmatrix} \quad (25b)$$

and

$$[R] = \begin{bmatrix} \sin \psi & -\cos \psi & 0 & 0 & 0 & 0 & 0 & 0 \\ \cos \psi & \sin \psi & 0 & 0 & 0 & 0 & 0 & 0 \\ 0 & 0 & 1 & 0 & 0 & 0 & 0 & 0 \\ 0 & 0 & 0 & 1 & 0 & 0 & 0 & 0 \\ 0 & 0 & 0 & 0 & \sin \psi & -\cos \psi & 0 & 0 \\ 0 & 0 & 0 & 0 & \cos \psi & \sin \psi & 0 & 0 \\ 0 & 0 & 0 & 0 & 0 & 0 & 1 & 0 \\ 0 & 0 & 0 & 0 & 0 & 0 & 0 & 1 \end{bmatrix} \quad (26)$$

Substituting (25) into (23) gives

$$\{\alpha\} = [A_r] \{\delta_r\}^e = [A_r] [R] \{\delta\}^e = [A] \{\delta\}^e \quad (27)$$

where

$$[A] = [A_r] [R]$$

$$[A] = \begin{bmatrix} \sin \psi & -\cos \psi & 0 & 0 & 0 & 0 & 0 & 0 \\ -\frac{\sin \psi}{\ell} & \frac{\cos \psi}{\ell} & 0 & 0 & \frac{\sin \psi}{\ell} & -\frac{\cos \psi}{\ell} & 0 & 0 \\ \cos \psi & \sin \psi & 0 & 0 & 0 & 0 & 0 & 0 \\ -a_1 \sin \psi & a_1 \cos \psi & b_1 & 0 & a_1 \sin \psi & -a_1 \cos \psi & 0 & 0 \\ a_2 \sin \psi & -a_2 \cos \psi & & & -a_2 \sin \psi & a_2 \cos \psi & & \\ -\frac{3 \cos \psi}{\ell^2} & -\frac{3 \sin \psi}{\ell^2} & -2b_2 & 0 & \frac{+3 \cos \psi}{\ell^2} & \frac{+3 \sin \psi}{\ell^2} & -b_4 & 0 \\ -a_3 \sin \psi & a_3 \cos \psi & & & a_3 \sin \psi & -a_3 \cos \psi & & \\ \frac{+2 \cos \psi}{\ell^3} & \frac{+2 \sin \psi}{\ell^3} & b_3 & 0 & \frac{-2 \cos \psi}{\ell^3} & \frac{-2 \sin \psi}{\ell^3} & b_5 & 0 \\ 0 & 0 & 0 & 1 & 0 & 0 & 0 & 0 \\ 0 & 0 & 0 & -\frac{1}{\ell} & 0 & 0 & 0 & \frac{1}{\ell} \end{bmatrix} \quad (28)$$

Chapter 6

STRESS-STRAIN RELATIONS

For an axisymmetric shell of revolution subjected to axisymmetric loadings, the stress resultants and couples can be expressed as

$$\begin{Bmatrix} N_1 \\ N_2 \\ M_1 \\ M_2 \\ Q_1 \end{Bmatrix} = \begin{bmatrix} E_{11} & E_{12} & E_{13} & E_{14} & 0 \\ E_{21} & E_{22} & E_{23} & E_{24} & 0 \\ E_{31} & E_{32} & E_{33} & E_{34} & 0 \\ E_{41} & E_{42} & E_{43} & E_{44} & 0 \\ 0 & 0 & 0 & 0 & E_{55} \end{bmatrix} \begin{Bmatrix} e_1 \\ e_2 \\ \kappa_1 \\ \kappa_2 \\ -\gamma_1 \end{Bmatrix} . \quad (29)$$

The quantities are related to the principal curvilinear coordinate system with 1 as meridional direction and 2 as circumferential direction. Symbolically this can be written as

$$\{S\} = [E] \{\epsilon\} \quad (30)$$

where $[E]$ is the elasticity matrix. The detail derivation of $[E]$ is given in Appendix A.

Substituting (19) into (17) gives

$$\begin{aligned} \{\epsilon\} &= [\phi'] \{\alpha\} \\ &= [\phi'] [A] \{\delta\}^e = [B] \{\delta\}^e \end{aligned} \quad (31)$$

$$[B] = [\phi'][A]$$

Differentiating the displacement functions with respect to x gives

$$\frac{du_r}{dx} = \alpha_2$$

$$\frac{dw_r}{dx} = \alpha_4 + 2\alpha_5 x + 3\alpha_6 x^2$$

$$\frac{dy_r}{dx} = \alpha_8$$

$$\frac{d^2 w_r}{dx^2} = 2\alpha_5 + 6\alpha_6 x$$

$$\frac{d^2 u_r}{dx^2} = 0$$

Substituting these relations into equation (17) gives

$$e_1 = \alpha_2 \cos^2 \beta + (\alpha_4 + 2\alpha_5 x + 3\alpha_6 x^2) \cos \beta \sin \beta + \frac{1}{2}(x_c)^2$$

$$e_2 = \frac{1}{r} [(\alpha_1 + \alpha_2 x) \sin \psi + (\alpha_3 + \alpha_4 x + \alpha_5 x^2 + \alpha_6 x^3) \cos \psi]$$

$$\kappa_1 = -\cos^3 \beta (2\alpha_5 + 6\alpha_6 x) - \frac{2 \cos \beta \sin \beta}{R_1} (\alpha_4 + 2\alpha_5 x + 3\alpha_6 x^2)$$

$$+ \frac{\sin^2 \beta - \cos^2 \beta}{R_1} (\alpha_2) - \alpha_8 \cos \beta$$

$$\kappa_2 = -\frac{\cos \phi}{r} [\cos^2 \beta (\alpha_4 + 2\alpha_5 x + 3\alpha_6 x^2) - \sin \beta \cos \beta \alpha_2]$$

$$- \frac{\cos \phi}{r} (\alpha_7 + \alpha_8 x)$$

$$\gamma_1 = -(\alpha_7 + \alpha_8 x)$$

From these equations, the matrix $[\phi']$ may be obtained and may be split into two matrices $[\phi'^L]$ and $[\phi'^N]$ containing linear and nonlinear terms.

$$\begin{aligned}\{\epsilon\} &= [\phi'] \{\alpha\} \\ &= ([\phi'^L] + [\phi'^N]) \{\alpha\}\end{aligned}$$

where $[\phi'^L]$ is given by

$$[\phi'^L] = \left[\begin{array}{ccccccccc} 0 & \cos^2 \beta & 0 & \cos \beta \sin \beta & 2x \cos \beta \sin \beta & 3x^2 \sin \beta \cos \beta & 0 & 0 \\ \frac{\sin \alpha}{r} & \frac{x \sin \alpha}{r} & \frac{\cos \alpha}{r} & \frac{x \cos \alpha}{r} & \frac{x^2 \cos \alpha}{r} & \frac{x^3 \cos \alpha}{r} & 0 & 0 \\ 0 & \frac{\sin^2 \alpha - \cos^2 \alpha}{R_1} & 0 & \frac{-2 \cos \alpha \sin \alpha}{R_1} & \frac{-4x \cos \alpha \sin \alpha}{R_1} & \frac{-6x^2 \cos \alpha \sin \alpha}{R_1} & 0 & -\cos \beta \\ 0 & \frac{\cos \alpha \sin \alpha \cos \beta}{r} & 0 & \frac{-\cos \alpha \cos \beta}{r} & \frac{-2x \cos \alpha \cos \beta}{r} & \frac{-3x^2 \cos \alpha \cos \beta}{r} & \frac{-\cos \alpha}{r} & \frac{-x \cos \beta}{r} \\ 0 & 0 & 0 & 0 & 0 & 0 & -1 & -x \end{array} \right] \quad (32)$$

and the non-zero first row of $[\phi'^N]$ is

$$[\phi'^N]_1 = \left[0 \quad \frac{-\sin \beta \cos \beta}{2} x \quad 0 \quad \frac{\cos^2 \beta}{2} x \quad x \cos^2 \beta x \quad \frac{3}{2} x^2 \cos^2 \beta x \quad 0 \quad 0 \right] \quad (32a)$$

The subscript 1 is used to denote the first row of the matrix.

From Equations (13) and (21)

$$\{f_r\} = [\phi] \{\alpha\} = [\phi] [A] \{\delta\}^e$$

$$\{f\} = [q_r]^{-1} \{f_r\} = [q_r]^T \{f_r\} \quad (33)$$

$$\{f\} = [q_r]^T [\phi] [A] \{\delta\}^e$$

$$= [N] \{\delta\}^e$$

where

$$[N] = [q_r]^T [\phi] [A] \quad . \quad (34)$$

The element stiffness matrix and equivalent nodal force may be obtained from the following formulas:

$$[k^e] = \iint_{A_e} [B]^T [E] [B] dA \quad (35)$$

$$\{F_p^e\} = \iint_{A_e} [N]^T \{P\} dA \quad (36)$$

where $\{P\}$ is the surface traction vector. The derivation of Equations (35) and (36) is given in Appendix B.

$$[\phi]^T = \begin{bmatrix} 1 & 0 & 0 & 0 \\ x & 0 & -sc & 0 \\ 0 & 1 & 0 & 0 \\ 0 & x & c^2 & 0 \\ 0 & x^2 & 2 \cdot x \cdot c^2 & 0 \\ 0 & x^3 & 3 \cdot x^2 \cdot c^2 & 0 \\ 0 & 0 & 0 & 1 \\ 0 & 0 & 0 & x \end{bmatrix} \quad (37)$$

$$[q_r] = \begin{bmatrix} \sin \psi & -\cos \psi & 0 & 0 \\ \cos \psi & \sin \psi & 0 & 0 \\ 0 & 0 & 1 & 0 \\ 0 & 0 & 0 & 1 \end{bmatrix} \quad (38)$$

$$[\phi]^T [q_r] = \begin{bmatrix} \sin \psi & -\cos \psi & 0 & 0 \\ x \sin \psi & -x \cos \psi & -sc & 0 \\ \cos \psi & \sin \psi & 0 & 0 \\ x \cos \psi & x \sin \psi & c^2 & 0 \\ x^2 \cos \psi & x^2 \sin \psi & 2x c^2 & 0 \\ x^3 \cos \psi & x^3 \sin \psi & 3x^2 c^2 & 0 \\ 0 & 0 & 0 & 1 \\ 0 & 0 & 0 & x \end{bmatrix} \quad (39)$$

$$\{p_r\} = \begin{Bmatrix} p_x \\ p_y \\ 0 \end{Bmatrix} \quad (40)$$

where

$$p_x = p_t \cos \beta - p_n \sin \beta$$

$$p_y = p_t \sin \beta + p_n \cos \beta .$$

$$\{p_r\} = [q_r]^T \{p\} \quad (41)$$

$$\{p\} = [q_r]^T \{p_r\} \quad (42)$$

$$= \begin{bmatrix} \sin \psi & \cos \psi & 0 & 0 \\ -\cos \psi & \sin \psi & 0 & 0 \\ 0 & 0 & 1 & 0 \\ 0 & 0 & 0 & 1 \end{bmatrix} \begin{Bmatrix} p_x \\ p_y \\ 0 \\ 0 \end{Bmatrix} \quad (43)$$

$$= \begin{Bmatrix} p_x \sin \psi + p_y \cos \psi \\ -p_x \cos \psi + p_y \sin \psi \\ 0 \\ 0 \end{Bmatrix} \quad (44)$$

$$\{z\}^T \{q_r\} \{p\} = \left\{ \begin{array}{l} p_x \sin^2 \psi + p_y \cos \psi \sin \psi + p_x \cos^2 \psi - p_y \sin \psi \cos \psi \\ p_x x \sin^2 \psi + p_y x \cos \psi \sin \psi + p_x x \cos^2 \psi - p_y x \cos \psi \sin \psi \\ p_x \cos \psi \sin \psi + p_y \cos^2 \psi - p_x \cos \psi \sin \psi + p_y \sin^2 \psi \\ p_x x \cos \psi \sin \psi + p_y x \cos^2 \psi - p_x x \sin \psi \cos \psi + p_y \sin^2 \psi \\ p_x x^2 \sin \psi \cos \psi + p_y x^2 \cos^2 \psi - p_x x^2 \sin \psi \cos \psi + p_y x^2 \sin^2 \psi \\ p_x x^3 \sin \psi \cos \psi + p_y x^3 \cos^2 \psi - p_x x^3 \sin \psi \cos \psi + p_y x^3 \sin^2 \psi \\ 0 \\ 0 \end{array} \right\} \quad (45)$$

$$= \left\{ \begin{array}{l} p_x \\ p_x x \\ p_y \\ p_y x \\ p_y x^2 \\ p_y x^3 \\ 0 \\ 0 \end{array} \right\} \quad (46)$$

This value may now be substituted into equations (34) and (36) to obtain $\{F_p^e\}$.

Chapter 7

RESULTS AND CONCLUSIONS

NUMERICAL EXAMPLES

To demonstrate the numerical accuracy of the method, some selected problems were solved and compared to known results.

First, a circular, monolithic, thin plate with clamped edges and subjected to a uniformly distributed load was considered. The plate had a radius of 100 inches and a thickness of 1.0 inch. Young's modulus was 1×10^6 psi and Poisson's ratio was 0.3. The plate was divided into five elements.

Using only five elements, the results from this program agree to within 7% of the exact results using large deflection theory shown in [20]. For the particular loading case, elementary theory differs from the exact solution by over 70%. The results are shown in Figure 2.

A comparison with Klein's [12] solution using linear analysis is shown in Figure 3. This was the analysis of a circular, flat plate under axisymmetric pressure loading. It can be seen that as the number of elements increased in the linear solution, it approached the nonlinear solution using only five elements.

A hemispherical shell is shown in Figure 4. A comparison was made with the theoretical values presented in [2]. The values calculated using the ORTHO2 program agreed with the theoretical values within the accuracy with which the curves could be read.

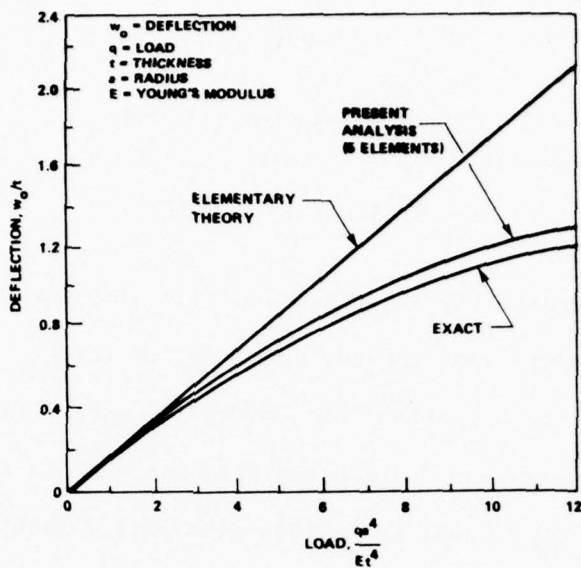


Figure 2. Circular Plate, Large Deflections.

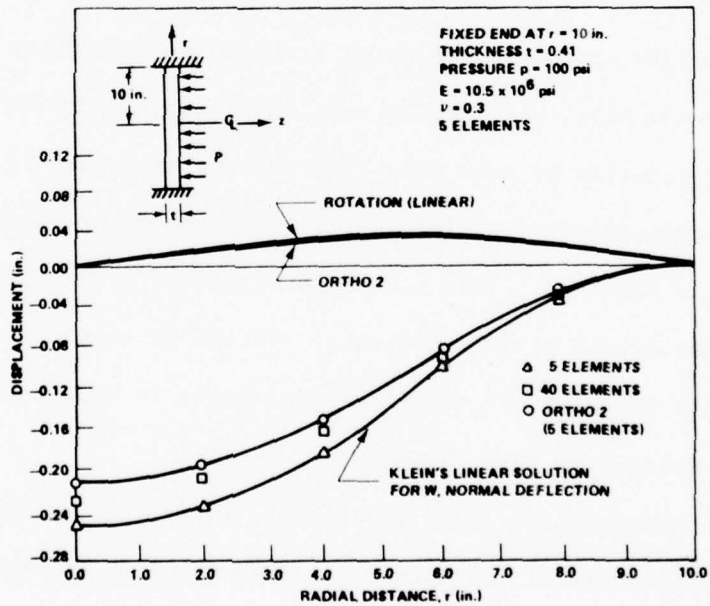


Figure 3. Circular Flat Plate Under Axisymmetric Pressure Loading.

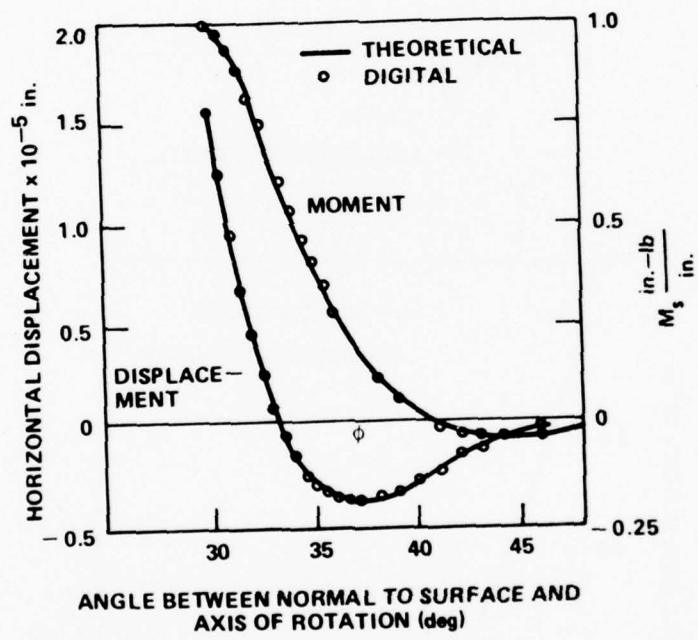
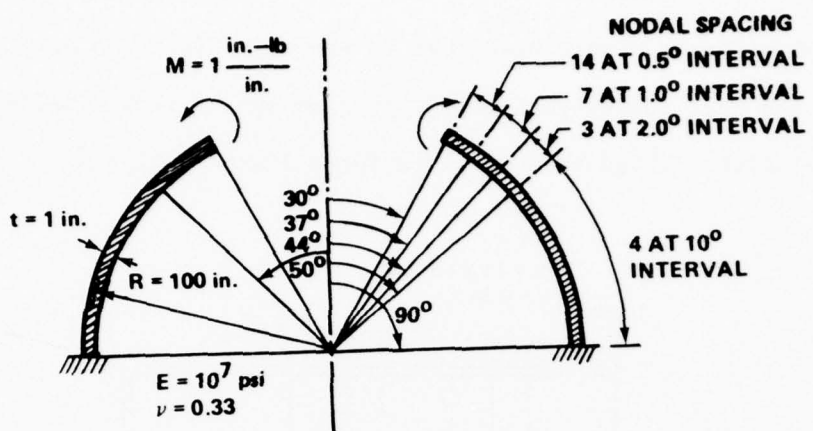


Figure 4. A Hemispherical Shell Solution by Finite Elements
(Grafton and Strome, J.A.I.A.A., 1963).

The radial deflection and meridional moment for a cylindrical shell subjected to a unit edge load is shown in Figures 5 and 6. It can be seen that the present ORTHO2 program agrees very closely with the exact solution. These solutions are for a linear analysis.

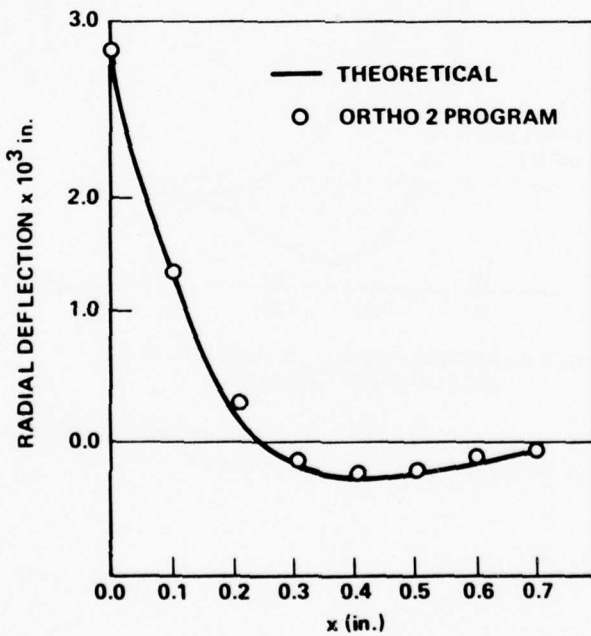
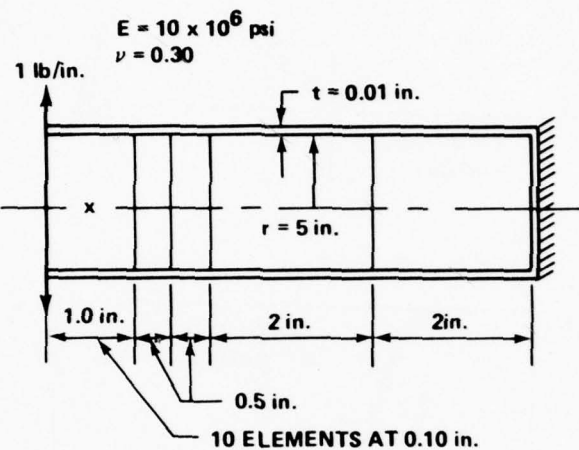


Figure 5. Cylindrical Shell with Unit Edge Load.

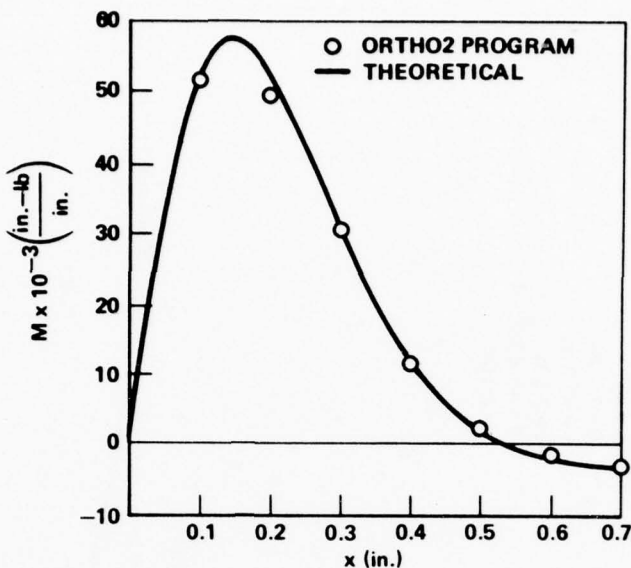


Figure 6. Meridional Moment for the Cylindrical Shell.

A spherical shell under uniform normal pressure was analyzed.

The shell and its properties are shown in Figure 7. A comparison was made with the exact solution given by [18]. It is readily seen that the present solution agrees with the exact solution very well.

The numerical influence of the shear deformation becomes much clearer when a circular sandwich plate with clamped edges subjected to a distributed load of 14 psi is considered. The plate has a radius of 10 in., the thickness of core layer is 0.75 in., and the thickness of upper and lower facings is 0.028 in. and 0.022 in., respectively. Young's modulus of facings is 10^7 psi, Poisson's ratio is 0.3, and the shear modulus of core is 30,000 psi. The plate is also divided into 5, 10, and 20 elements. The results are given in Figure 8. The maximum deflection of the plate is shown to converge to the theoretical value of 0.0415 in. as reported by Plantema [19].

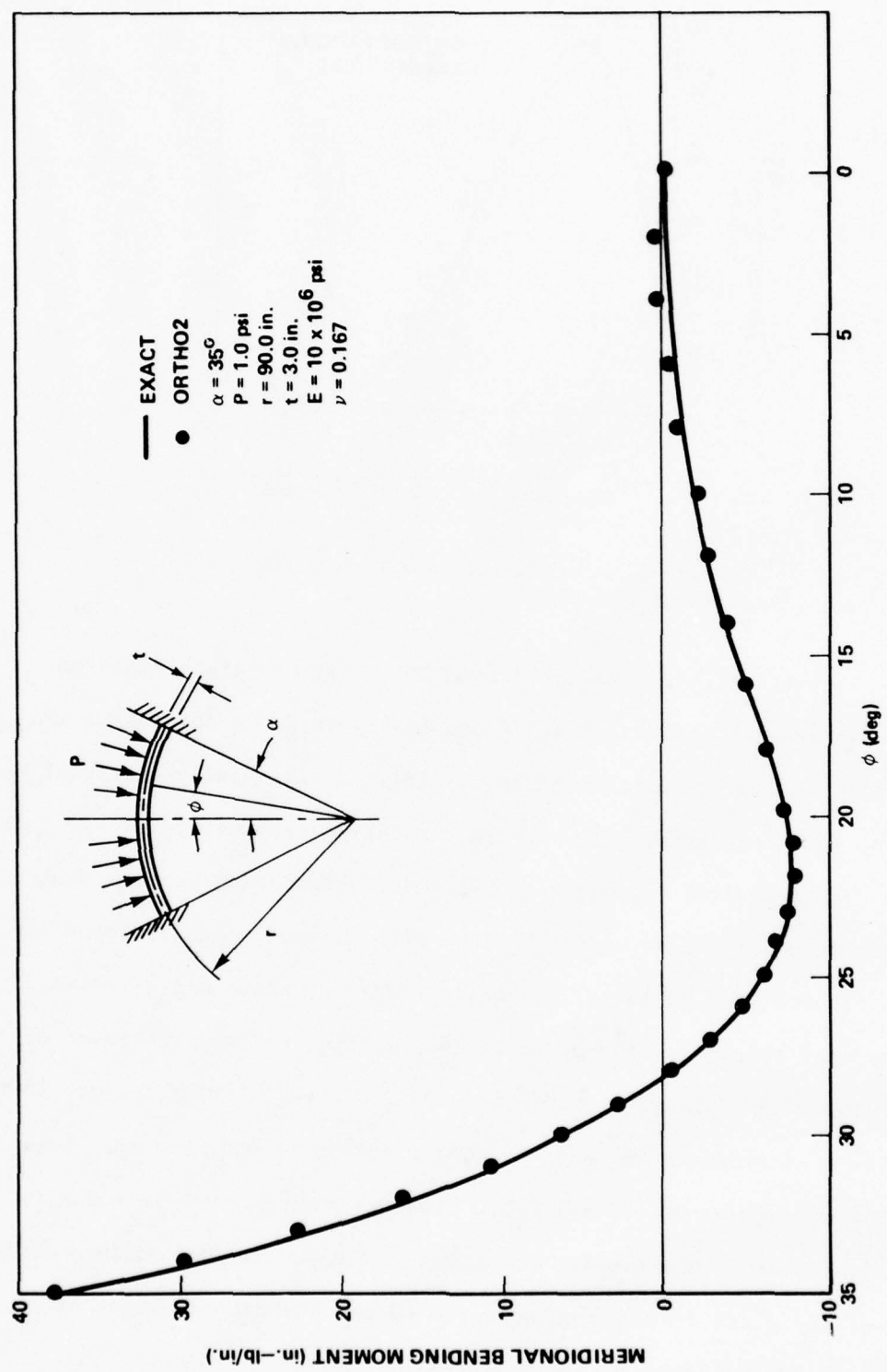


Figure 7. Meridional Bending Moment.

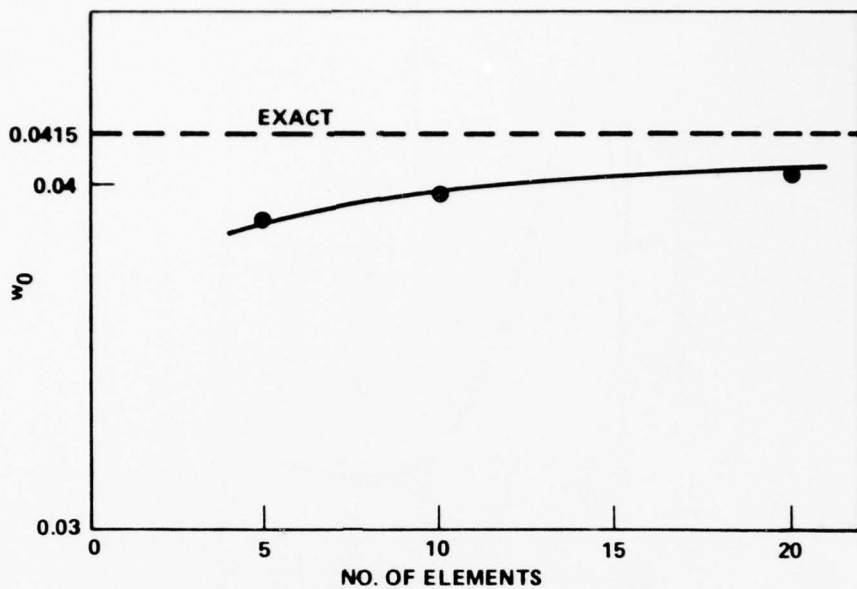


Figure 8. Convergence of Center Deflection of Circular Sandwich Plate.

Nickell [14] obtained a solution for a cylinder loaded with a radial load on one end and a moment (see Figure 9). The results are compared with the present solutions in Figures 10 through 12. The results agree with Nickell's within the limits of accuracy with which the curves can be read.

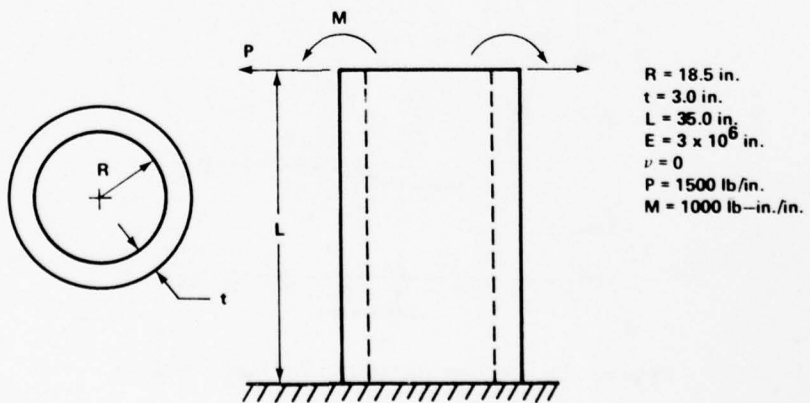


Figure 9. Locally Loaded Cylinder.

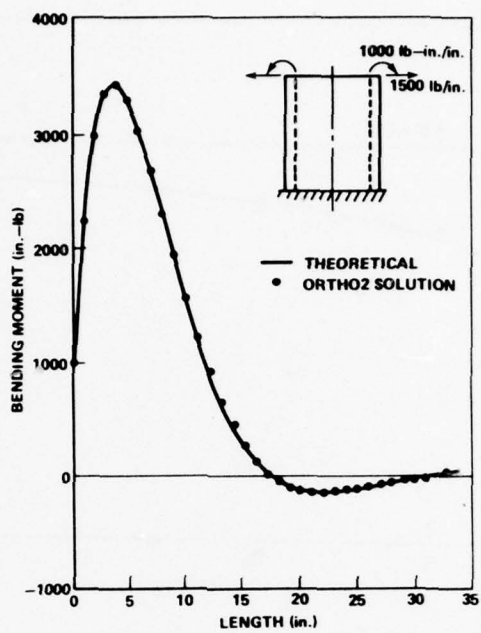


Figure 10. Bending Moment Versus Length.

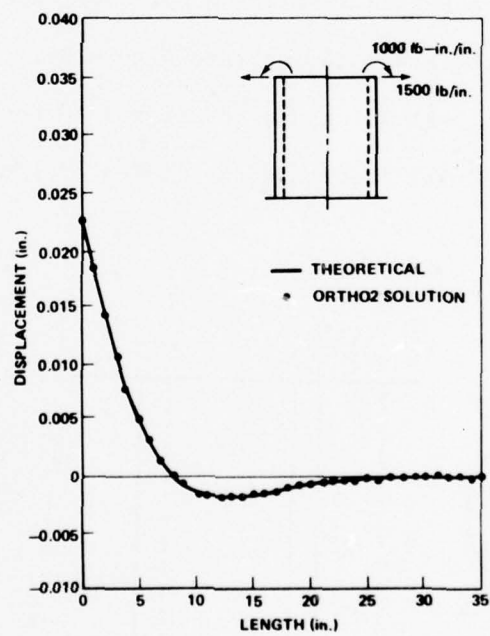


Figure 11. Displacement Versus Length.

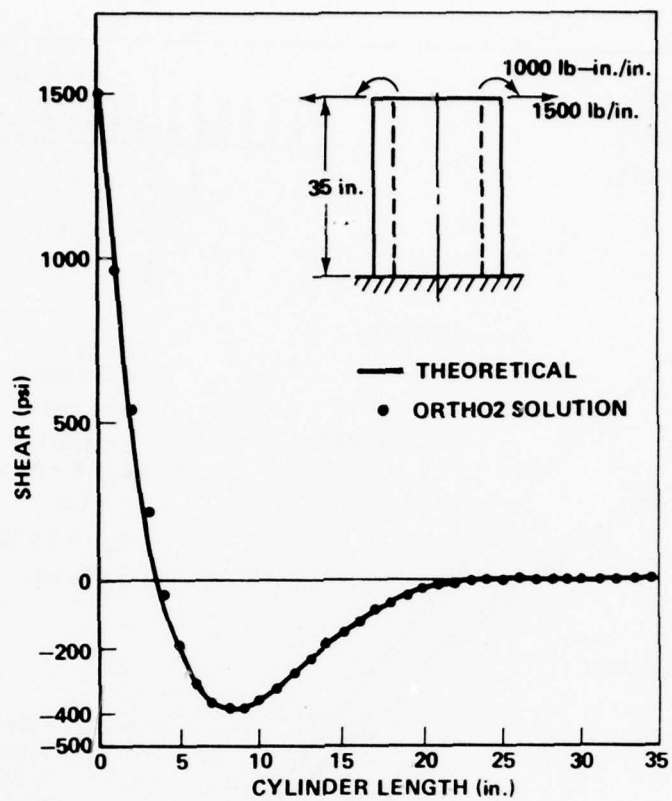


Figure 12. Shear Versus Length.

Sharifi [13] analyzed a clamped circular sandwich plate under a uniform lateral pressure. A comparison with his solution and the linear solution is shown in Figure 13. He used an incremental formulation for a nonlinear finite element analysis of sandwich structures. The nonlinearities considered were due to large displacements, as a result of finite rotations, and plastic deformations of the facings. The ORTHO2 program solution agreed very closely with these results as evidenced in Figure 13. The nonlinear solution differs significantly from the linear.

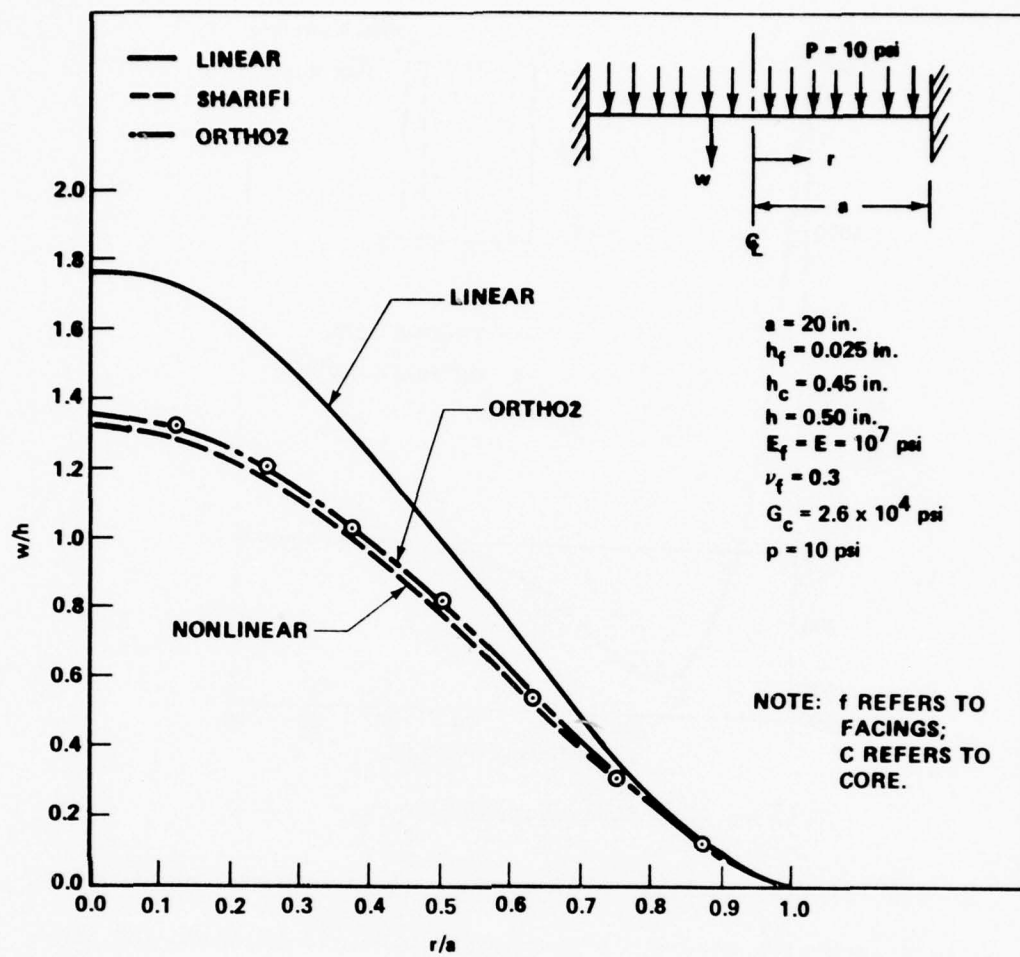


Figure 13. Transverse Deflections in a Clamped Circular Sandwich Plate.

CONCLUSIONS

A method for performing a nonlinear analysis on an orthotropic, laminated shell of revolution has been presented. The shell was assumed to be torsion-free. The classical Kirchhoff-Love assumption for normals to the midsurface was relaxed in favor of the assumed shear deformation. The method is quite general and applicable to any shell geometry possessing axial symmetry.

A finite element method that used the displacement model was selected to analyze the system. The meridional curve of the shell was represented by a series of curved elements having local coordinates. An element was developed that matches slopes and curvatures as well as displacements at its nodal circle.

The geometric approximation of curved shells usually associated with the finite element method is minimized by using the curved element. The use of this curved element significantly reduces the meridional bending moment usually present at the nodal circles when a curved structure is approximated by a straight line (conical) segment. A smaller number of elements can be used in comparison to that of a conical element.

A computer program was developed to solve the derived equations. The program was shown to be a versatile and flexible method of implementing the basic theory. Several problems were solved and the results compared with both linear and nonlinear solutions from the literature. In most cases, the results from this program agreed with the linear solutions within the limits of accuracy with which the curves could be read. Agreement with nonlinear solutions was good and could usually be further improved by taking more elements. The shell thickness and pressure may vary linearly along the meridian. The convergence and accuracy of the method were found to be entirely satisfactory as evidenced by the numerical examples.

The Gaussian Quadrature Integration method was used in the derivation of the stiffness matrix. Several tests were made to determine the most efficient method. As many as eight points were used. After

examining the different schemes, it was decided that the two point Gaussian Integration scheme gave the best results.

The accuracy obtained by this method depends directly on the extent to which the assumed displacement patterns are able to reproduce the deformation actually developed within the element. Since the chosen displacement patterns satisfy the requirements of completeness and conformity (continuity of displacement at element boundary) as the size of the element decreases indefinitely, the solution obtained converges to the exact solution.

The finite element method is obviously a powerful tool in the analysis of orthotropic, composite structures. There still remains much work to do in this area. A logical extension of this work is to include stability criteria. Other items which should be considered in the future are: crossover effects, cracking or "crazing" of the matrix material, an appropriate failure criterion, and material properties which are different in tension and compression.

Appendix A

ELASTICITY MATRIX

Individual curved finite elements can, in general, be composed of a number of anisotropic layers of varying thickness along the meridional coordinate. For a single lamina, considering shear deformations, the constitutive relation is given as

$$\begin{Bmatrix} \sigma_L \\ \sigma_T \\ \tau_{LT} \\ \tau_{L\zeta} \\ \tau_{T\zeta} \end{Bmatrix} = \begin{bmatrix} Q'_{11} & Q'_{12} & 0 & 0 & 0 \\ Q'_{12} & Q'_{22} & 0 & 0 & 0 \\ 0 & 0 & Q'_{44} & 0 & 0 \\ 0 & 0 & 0 & Q'_{55} & 0 \\ 0 & 0 & 0 & 0 & Q'_{66} \end{bmatrix} \begin{Bmatrix} \epsilon_L \\ \epsilon_T \\ \gamma_{LT} \\ \gamma_{L\zeta} \\ \gamma_{T\zeta} \end{Bmatrix} \quad (A-1)$$

where the transverse normal stress σ_ζ has been omitted and the laminae are orthotropic with respect to the principal elastic axes L-T. These axes need not coincide with the axes of the curvilinear coordinate system 1-2, (Figure 14), (1 is the meridional direction) and

$$Q'_{11} = E_L / (1 - v_{LT} v_{TL})$$

$$Q'_{12} = v_{LT} E_T / (1 - v_{LT} v_{TL})$$

$$= v_{TL} E_L / (1 - v_{TL} v_{LT})$$

$$Q'_{22} = E_T / (1 - \nu_{LT} \nu_{TL})$$

$$Q'_{44} = G_{LT}$$

(A-2)

$$Q'_{55} = G_{L\zeta}$$

$$Q'_{66} = G_{T\zeta}$$

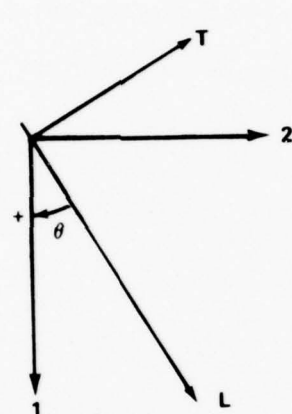


Figure 14. Material Axes.

Equation (A-1) can also be written for the k th layer in the following forms:

$$\begin{Bmatrix} \sigma_L \\ \sigma_T \\ \tau_{LT} \end{Bmatrix}_k = \begin{bmatrix} Q'_{11} & Q'_{12} & 0 \\ Q'_{12} & Q'_{22} & 0 \\ 0 & 0 & Q'_{44} \end{bmatrix}_k \begin{Bmatrix} \epsilon_L \\ \epsilon_T \\ \gamma_{LT} \end{Bmatrix}$$
(A-3)

and

$$\begin{Bmatrix} \tau_{L\zeta} \\ \tau_{T\zeta} \end{Bmatrix}_k = \begin{bmatrix} Q'_{55} & 0 \\ 0 & Q'_{66} \end{bmatrix}_k \begin{Bmatrix} \gamma_{L\zeta} \\ \gamma_{T\zeta} \end{Bmatrix}_k$$

To develop a theory for structural laminates with individual layers having their elastic axes oriented at various angles relative to the coordinate axes, the stress-strain Equations (A-3) must be rotated through the positive angle θ so that the transformed stress-strain equations are

$$\begin{Bmatrix} \sigma_1 \\ \sigma_2 \\ \tau_{12} \end{Bmatrix}_k = \begin{bmatrix} \bar{Q}_{11} & \bar{Q}_{12} & \bar{Q}_{14} \\ \bar{Q}_{12} & \bar{Q}_{22} & \bar{Q}_{24} \\ \bar{Q}_{14} & \bar{Q}_{24} & \bar{Q}_{44} \end{bmatrix}_k \begin{Bmatrix} \epsilon_1 \\ \epsilon_2 \\ \gamma_{12} \end{Bmatrix}_k \quad (A-4)$$

and

$$\begin{Bmatrix} \tau_{1\zeta} \\ \tau_{2\zeta} \end{Bmatrix}_k = \begin{bmatrix} \bar{Q}_{55} & 0 \\ 0 & \bar{Q}_{66} \end{bmatrix}_k \begin{Bmatrix} \gamma_{1\zeta} \\ \gamma_{2\zeta} \end{Bmatrix}_k$$

where

$$\begin{aligned} \bar{Q}_{11} &= Q'_{11} \cos^4 \theta + 2(Q'_{12} + 2 Q'_{44}) \sin^2 \theta \cos^2 \theta + Q'_{22} \sin^4 \theta \\ \bar{Q}_{12} &= (Q'_{11} + Q'_{22} - 4 Q'_{44}) \sin^2 \theta \cos^2 \theta + Q'_{12} (\sin^4 \theta + \cos^4 \theta) \\ \bar{Q}_{22} &= Q'_{11} \sin^4 \theta + 2(Q'_{12} + 2 Q'_{44}) \sin^2 \theta \cos^2 \theta + Q'_{22} \cos^4 \theta \\ \bar{Q}_{14} &= (Q'_{11} + Q'_{12} - 2 Q'_{44}) \sin \theta \cos^3 \theta + (Q'_{12} - Q'_{22} + 2 Q'_{44}) \sin^3 \theta \cos \theta \\ \bar{Q}_{24} &= (Q'_{11} - Q'_{12} - 2 Q'_{44}) \sin^3 \theta \cos \theta + (Q'_{12} - Q'_{22} + 2 Q'_{44}) \sin \theta \cos^3 \theta \\ \bar{Q}_{44} &= (Q'_{11} + Q'_{22} - 2 Q'_{12} - 2 Q'_{44}) \sin^2 \theta \cos^2 \theta + Q'_{44} (\sin^4 \theta \cos^4 \theta) \\ \bar{Q}_{55} &= Q'_{55} \\ \bar{Q}_{66} &= Q'_{66} \end{aligned} \quad (A-5)$$

Substituting the midsurface strain and curvatures into Equations (A-4) the following expression is obtained:

$$\begin{Bmatrix} \sigma_1 \\ \sigma_2 \\ \tau_{12} \end{Bmatrix}^e = [\bar{Q}]_k \begin{Bmatrix} e_1 \\ e_2 \\ 2e_{12} \end{Bmatrix} + \zeta [\bar{Q}]_k \begin{Bmatrix} \kappa_1 \\ \kappa_2 \\ 2\kappa_{12} \end{Bmatrix} \quad (A-6)$$

and

$$\begin{Bmatrix} \tau_{1\zeta} \\ \tau_{2\zeta} \end{Bmatrix} = \begin{bmatrix} \bar{Q}_{55} & 0 \\ 0 & \bar{Q}_{66} \end{bmatrix} \begin{Bmatrix} \gamma_{1\zeta} \\ \gamma_{2\zeta} \end{Bmatrix}$$

By integrating over the total thickness of the laminate, the generalized stress resultants in terms of midsurface strain and curvature are given as

$$\begin{Bmatrix} N_1 \\ N_2 \\ N_{12} \\ M_1 \\ M_2 \\ M_{12} \\ Q_1 \\ Q_2 \end{Bmatrix} = \begin{bmatrix} [C] & [D^*] & 0 \\ [D^*] & [D] & 0 \\ 0 & 0 & [S] \end{bmatrix} \begin{Bmatrix} e_1 \\ e_2 \\ 2e_{12} \\ \kappa_1 \\ \kappa_2 \\ 2\kappa_{12} \\ \gamma_{1\zeta} \\ \gamma_{2\zeta} \end{Bmatrix} \quad (A-7)$$

where

$$\begin{aligned}
 [C] &= \sum_{k=1}^m [\bar{Q}^{(k)}] (h_k - h_{k-1}) \\
 [D^*] &= \frac{1}{2} \sum_{k=1}^m [\bar{Q}^{(k)}] (h_k^2 - h_{k-1}^2) \\
 [D] &= \frac{1}{3} \sum_{k=1}^m [\bar{Q}^{(k)}] (h_k^3 - h_{k-1}^3) \\
 [S] &= \sum_{k=1}^m [\bar{Q}^{(k)}] (h_k - h_{k-1})
 \end{aligned} \tag{A-8}$$

in which h_k and h_{k-1} = the distances, respectively, from the midsurface to the inner and outer surfaces of the k -th layer.

For an axisymmetric shell of revolution subjected to axisymmetric loadings, $N_{12} = M_{12} = Q_2 = e_{12} = \kappa_{12} = \gamma_{2\zeta} = 0$.

Hence,

$$\left\{ \begin{array}{c} N_1 \\ N_2 \\ M_1 \\ M_2 \\ Q_1 \end{array} \right\} = \left[\begin{array}{ccc} [C] & [D^*] & 0 \\ [D^*] & [D] & 0 \\ 0 & 0 & S_{55} \end{array} \right] \left\{ \begin{array}{c} e_1 \\ e_2 \\ \kappa_1 \\ \kappa_2 \\ \gamma_{1\zeta} \end{array} \right\} \tag{A-9}$$

or symbolically

$$\{S\} = [E] \{e\} \quad . \tag{A-10}$$

Appendix B

ELEMENT STIFFNESS MATRIX

The element stiffness matrix is found by writing the total potential energy of the axisymmetric shell of revolution and minimizing it for the imposed constraints and loading conditions.

The potential energy for a linear elastic shell of revolution in the absence of thermal and body forces can be formulated as follows:

$$\pi = \iiint_V \frac{1}{2} \{\epsilon\}^T \{\sigma\} dV - \iint_{A_1} \{f\}^T \{P\} dA \quad (B-1)$$

where the vectors $\{\epsilon\}$, $\{\sigma\}$, $\{f\}$, and $\{P\}$ represent the strain, stress, displacement, and equivalent surface traction vectors, respectively.

Introducing the stress resultant vector

$$\{S\} = t \{\sigma\} \quad (B-2)$$

where t is the thickness of the shell, Equation (B-1) may be written as

$$\pi = \iiint_V \frac{1}{2} \{\epsilon\}^T \{S\} \frac{dV}{t} - \iint_{A_1} \{f\}^T \{P\} dA . \quad (B-3)$$

The first integral is evaluated over the entire volume V of the shell and the second over the portion A_1 of the midsurface of the shell, where the equivalent surface tractions are prescribed. Since the state of displacement throughout the shell is defined element by element, the

total potential energy may be considered as the sum of the potential energies of all individual elements, i.e.,

$$\pi = \sum_e \pi^e .$$

The potential energy contribution of element "e" will now be considered. The state of displacement defined for the element in local rectilinear coordinates x-y can be expressed in matrix form in Equation (21) as

$$\{f_r\} = [\phi] \{\alpha\} = [\phi][A_r] \{\delta_r^e\} . \quad (B-4)$$

Transformation of $\{f_r\}$ into the global coordinate system may be obtained from Equation (13)

$$\{f\} = [q_r]^T \{f_r\} = [N] \{\delta_r^e\} \quad (B-5)$$

where

$$[N] = [q_r]^T [\phi] [A_r] \quad (B-6)$$

and the column vector $\{\delta_r^e\}$ represents the eight discrete parameters (nodal point displacements) of the element as given in Equation (25b). The matrix [N] is a function of spatial coordinates and describes the defined displacement pattern.

Substituting Equation (27) into Equation (31) the following strain-displacement relations are obtained:

$$\{\epsilon\} = [B] \{\delta\}^e \quad (B-7)$$

where

$$[B] = [\phi'] [A] . \quad (B-8)$$

Equation (B-8) is a matrix relating the nodal point displacement vector to the strain vector. The elastic stress-strain relations can be expressed as

$$\{S\} = [E] \{\epsilon\} \quad (B-9)$$

where $[E]$ is a function of the elastic properties of the element. Each element can be assigned different elastic properties. If the relations in Equations (B-9), (B-5), and (B-7) are substituted into (B-3), the potential energy contribution for the element becomes

$$\pi^e = \iiint_{V_e} \frac{1}{2} \{\delta^e\}^T [B]^T [E] [B] \{\delta^e\} \frac{dV}{t} - \iint_{A_{1_e}} \{\delta^e\}^T [N]^T \{P\} dA \quad (B-10)$$

where V_e is the volume of the element and A_{1_e} is that part of the mid-surface area of the element which coincides with the midsurface area A_1 of the shell over which the equivalent surface tractions are prescribed.

Since the discrete parameters $\{\delta^e\}$ are not a function of spatial coordinates, the potential energy of the element may be written as

$$\pi^e = \{\delta^e\}^T \left[\iiint_{V_e} \frac{1}{2} [B]^T [E][B] \frac{dV}{t} \right] \{\delta^e\} - \{\delta^e\}^T \iint_{A_{1_e}} [N]^T \{P\} dA . \quad (B-11)$$

Since the assumed displacement patterns for each element satisfy various requirements such as completeness and conformity, the best values that can be obtained for the total nodal point displacements of the finite element representation of shells of revolution are those

that minimize the total potential energy of the shell under the constraints imposed; i.e., the best value of $\{\delta\}$ are those that satisfy the system of linear equations

$$\frac{\partial \pi}{\partial \{\delta\}} = 0 \quad (B-12)$$

where $\{\delta\}$ is the total nodal displacement vector of the system.

In forming the system of Equations (B-12), it is convenient to have an expression for the spatial derivatives of the potential energy of each element "e" with respect to its own nodal point displacement vector $\{\delta^e\}$, i.e.,

$$\frac{\partial \pi^e}{\partial \{\delta^e\}} = \left[\frac{\partial \pi^e}{\partial u_I} \frac{\partial \pi^e}{\partial w_I} \frac{\partial \pi^e}{\partial x_I} \frac{\partial \pi^e}{\partial \gamma_I} \frac{\partial \pi^e}{\partial u_J} \frac{\partial \pi^e}{\partial w_J} \frac{\partial \pi^e}{\partial x_J} \frac{\partial \pi^e}{\partial \gamma_J} \right] . \quad (B-13)$$

By use of Equation (B-10), this expression can be obtained as

$$\frac{\partial \pi^e}{\partial \{\delta^e\}} = \left[\iiint_{V_e} [B]^T [E][B] \frac{dv}{t} \right] \{\delta^e\} - \left[\iint_{A_{1_e}} [N]^T \{P\} dA \right] . \quad (B-14)$$

The terms in the first and second brackets are normally defined as the element stiffness matrix $[K^e]$ and the element generalized nodal point force $\{F^e\}$, respectively. Hence,

$$[K^e] = \iiint_{V_e} [B]^T [E][B] \frac{dv}{t} \quad (B-15)$$

$$\{F^e\} = \iint_{A_{1_e}} [N]^T \{P\} dA . \quad (B-16)$$

By properly combining the submatrices in Equation (B-14) obtained for each element, the total matrix equation representing Equation (B-12) can be constructed as

$$[K] \{ \delta \} = \{ F \} \quad (B-17)$$

and then solved for the nodal point displacements. Once the nodal point displacements are obtained, the corresponding stress resultants, stresses, and strains for the defined displacement patterns can be calculated from Equations (B-7) and (B-9).

If Equation (B-8) is substituted into Equation (B-15) and the volume increment for a shell of revolution is taken as

$$dV = 2\pi t \frac{R(x)}{\cos \beta} dx , \quad (B-18)$$

then the element stiffness matrix for the axisymmetric shell element takes the form

$$\begin{aligned} [K^e] &= 2\pi \int_0^\ell [B]^T [E][B] \frac{R(x)}{\cos \beta} dx \\ &= 2\pi [A]^T [G][A] \end{aligned} \quad (B-19)$$

where

$$[G] = \int_0^\ell [\phi']^T [E][\phi'] \frac{R(x)}{\cos \beta} dx . \quad (B-20)$$

The integration is over the chord length of the meridian cross section of element.

It is assumed that the equivalent surface traction over the mid-surface area A_1 where tractions are prescribed varies linearly between the two nodal circles I and J. That is,

$$\{P_c\}^T = [0 \ (P_n + P'_n x) \ 0 \ 0] \quad (B-21)$$

where $\{P_c\}$ is the surface traction vector expressed in local curvilinear coordinates. Transforming into global coordinates the following is obtained:

$$\{P\} = [q_r]^T [q_c]^T \{P_c\} \quad . \quad (B-22)$$

Substituting Equations (B-6) and (B-22) into Equation (B-16) the generalized element nodal force vector becomes

$$\{F^e\} = 2\pi \int_0^\ell [A_r]^T [\phi]^T [q_r][q_c]^T \{P_c\} \frac{R(x)}{\cos \beta} dx \quad (B-23)$$

or

$$\{F^e\} = 2\pi[A_r]^T \int_0^\ell [\phi]^T [q_c]^T \{P_c\} \frac{R(x)}{\cos \beta} dx$$

where

$$[\phi]^T [q_c]^T \{P_c\} = P_n \left\{ \begin{array}{l} -\sin \beta \\ -x \sin \beta \\ \cos \beta \\ x \cos \beta \\ x^2 \cos \beta \\ x^3 \cos \beta \\ 0 \\ 0 \end{array} \right\} + P'_n \left\{ \begin{array}{l} -x \sin \beta \\ -x^2 \sin \beta \\ x \cos \beta \\ x^2 \cos \beta \\ x^3 \cos \beta \\ x^4 \cos \beta \\ 0 \\ 0 \end{array} \right\} .$$

Appendix C

EQUILIBRIUM EQUATIONS BY VIRTUAL WORK

The equilibrium equations governing the shell behavior can be derived by using the principle of virtual work.

From Equations (21), (23), and (25a)

$$\begin{aligned}
 \{\bar{f}\} &= [\phi] \{\alpha\} \\
 &= [\phi] [\bar{A}] \{\bar{u}\} \\
 &= [\phi] [\bar{A}] [R] \{u_g\} \\
 &= [\phi] [A] \{u_g\} \\
 &= [N] \{u_g\}
 \end{aligned} \tag{C-1}$$

where $[N] = [\phi][A]$ and $[A] = [\bar{A}][R]$.

Let there be an arbitrary and non-zero virtual nodal displacement $\delta\{u_g\}$ about the deformed position which results in a virtual displacement $\delta\{\bar{f}\}$ and virtual strain $\delta\{\epsilon\}$. The δ prefix denotes a virtual change in the quantity concerned.

By means of the principle of virtual work, the following expression can be written:

$$\delta\{u_g\}^T \{Q\} = \int_{A_m} \delta\{\epsilon\}^T \{\tau\} dA_m - \int_{A_m} \delta\{\bar{f}\}^T \{F_s\} dA_m \tag{C-2}$$

where A_m is the reference surface area of the shell, $\{Q\}$ is the applied nodal force vector and $\{F_s\}$ is the surface traction vector. The stress

vector $\{\tau\}$ is given as

$$\begin{aligned}\{\tau\} &= [C]\{\epsilon\} \\ &= [C][\phi'][A]\{u_g\} \quad .\end{aligned}$$

Substituting Equation (C-1) into (C-2) the following is obtained:

$$\delta\{u_g\}^T \{Q\} + \delta\{u_g\}^T \int_{A_m} [N]^T \{F_s\} dA_m = \int_{A_m} \delta\{\epsilon\}^T \{\tau\} dA_m$$

or

$$\delta\{u_g\}^T \{P\} = \int_{A_m} \delta\{\epsilon\}^T \{\tau\} dA_m \quad (C-3)$$

where $\{P\}$ is the equivalent nodal forces of the element defined by the principle of virtual work.

Substituting Equations (23), (25a), and (31) into (C-3) gives:

$$\delta\{u_g\}^T \{P\} = \int_{A_m} \delta\{u_g\}^T [A]^T [\phi']^T \{\tau\} dA_m \quad . \quad (C-4)$$

This results in a nonlinear matrix equation for the equivalent nodal forces $\{P\}$, i.e.,

$$\{P\} = \int_{A_m} [A]^T [\phi']^T [C][\phi'][A] \{u_g\} dA_m \quad . \quad (C-5)$$

Equation (C-5) is now linearized by writing it in the form of an implicit differential.

$$\begin{aligned}
 \Delta \{P\} = & \int_{A_m} \Delta [A]^T [\phi']^T [C][\phi'][A] \{u_g\} dA_m \\
 & + \int_{A_m} [A]^T \Delta ([\phi']^T [C][\phi']) [A] \{u_g\} dA_m \quad (C-6) \\
 & + \int_{A_m} [A]^T [\phi'][C][\phi'][A] \Delta \{u_g\} dA_m .
 \end{aligned}$$

It is assumed that a change in the transformation matrix during an increment of load may be neglected. This permits neglecting the first term on the right hand side of equation (C-6). The second term results in the well known initial stress matrix while the third term accounts for the effect of the increment of strain and may be split into two terms separating the linear and nonlinear displacement terms.

$$\begin{aligned}
 & \int_{A_m} [A]^T [\phi']^T [C][\phi'][A] \Delta \{u_g\} dA_m = \\
 & \int_{A_m} [A]^T [\phi'^\ell]^T [C][\phi'^\ell][A] dA_m \Delta \{u_g\} + \\
 & \int_{A_m} [A]^T [\phi'^\ell]^T [C][\phi'^n][A] dA_m \Delta \{u_g\} + \\
 & \int_{A_m} [A]^T [\phi'^n]^T [C][\phi'^\ell][A] dA_m \Delta \{u_g\} + \\
 & \int_{A_m} [A]^T [\phi'^n]^T [C][\phi'^n][A] dA_m \Delta \{u_g\} = \\
 & \left([K^{(0)}] + [K^{(2)}] \right) \Delta \{u_g\} . \quad (C-7)
 \end{aligned}$$

The last three terms have been collected into $[K^{(2)}]$ and will be called the initial displacement matrix. If the area increment of the shell is taken as

$$dA_m = 2\pi \frac{R(x)}{\cos \beta} dx$$

then the element stiffness matrix for the axisymmetric shell element takes the form

$$\begin{aligned}[K^e] &= 2\pi \int_0^\ell [B]^T [C][B] R(x) dx \\ &= 2\pi [A]^T [G][A]\end{aligned}$$

where

$$[B] = [\phi'][A]$$

and

$$[G] = \int_0^\ell [\phi']^T [C][\phi'] R(x) dx .$$

The integration is over the chord length of the meridian cross section of element.

INITIAL STRESS MATRIX

The second term of Equation (C-6) can be written as:

$$\begin{aligned}\int_{A_m} [A]^T \Delta([\phi']^T [C][\phi']) [A] \{u_g\} dA_m &= \\ 2 \int_{A_m} [A]^T (\Delta[\phi']^T [C][\phi'][A]) \{u_g\} dA_m &= \\ 2 \int_{A_m} [A]^T (\Delta[\phi']^T) \{\tau\} dA_m .\end{aligned}\tag{C-8}$$

Equation (C-8) can be broken down into a summation of the five stress resultant components, i.e.,

$$2 \int_{A_m} [A]^T \Delta[\phi']^T \{ \tau \} dA_m = \sum_{i=1}^5 \int_{A_m} \tau_i [A]^T 2 \Delta \{ \phi_i^{nT} \} dA_m \quad (C-9)$$

where i is the index of the stress resultant components and $\{ \phi_i^{nT} \}$ is the transpose of the corresponding i^{th} row of the matrix $[\phi']$.

Since the derivation is based on the current deformed position of the shell element, the increment $\Delta \{ \phi_i^{nT} \}$ can be written as follows:

$$2 \Delta \{ \phi_i^{nT} \} = 2 \Delta \{ \phi_i^{nT} \} = 2 \Delta \{ \phi_1^{nT} \}$$

and

$$2 \Delta \{ \phi_1^{nT} \} = 2 \left\{ \frac{\partial \phi_1^{nT}}{\partial x} \right\} \Delta x$$

$$= \begin{Bmatrix} 0 \\ -\sin \beta \\ 0 \\ 1 \\ 2x \\ 3x^2 \\ 0 \\ 0 \end{Bmatrix} [0 \quad -\sin \beta \quad 0 \quad 1 \quad 2x \quad 3x^2 \quad 0 \quad 0] \Delta \{ x \}$$

Appendix D

THEORETICAL BACKGROUND

Some of the basic concepts used in the derivation of the equations presented in the main text are presented in this section.

GEOMETRY OF SHELLS

The geometry of a shell is entirely defined once the midsurface and the thickness at each point are specified. Hence, to describe the shell space, the middle surface or reference surface of the shell must be specified. Let α_1 and α_2 be the curvilinear coordinates for the mid-surface and let them coincide with lines of principal curvature of the surface, and let ζ be a coordinate normal to the midsurface as shown in Figure 15.

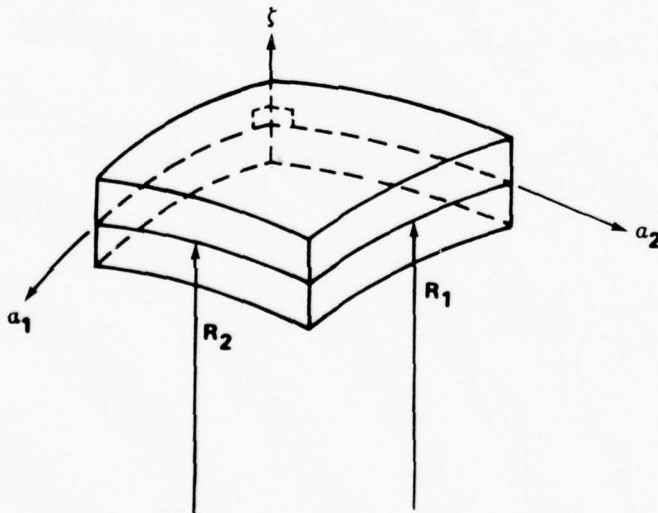


Figure 15. Typical Shell Element.

The position of any point in the midsurface can be defined by the curvilinear coordinates α_1 and α_2 . The location of any point in the shell can be related by the three parameters α_1 , α_2 , and ζ . With this curvilinear coordinate system, a line element in the shell space surrounding the midsurface can be expressed in terms of the differentials of the orthogonal curvilinear coordinates as follows:

$$ds^2 = A_1^2 \left(1 + \frac{\zeta}{R_1}\right)^2 d\alpha_1^2 + A_2^2 \left(1 + \frac{\zeta}{R_2}\right)^2 d\alpha_2^2 + d\zeta^2 \quad (D-1)$$

where A_1 and A_2 are the midsurface metrics and R_1 and R_2 are the principal radii of curvature of the surface.

STRAIN-DISPLACEMENT RELATIONSHIPS

The general nonlinear strain-displacement relations for large rotation but small strain were derived by Novozhilov [18] and later corrected by Tsao [19]. Suppressing the nonlinear terms, the following strain-displacement relations for linear theory of shells is obtained:

$$\begin{aligned} \epsilon_1 &= -\frac{1}{1 + \frac{\zeta}{R_1}} \left(\frac{1}{A_1} \frac{\partial U}{\partial \alpha_1} + \frac{V}{A_1 A_2} \frac{\partial A_1}{\partial \alpha_2} + \frac{W}{R_1} \right) \\ \epsilon_2 &= \frac{1}{1 + \frac{\zeta}{R_2}} \left(\frac{1}{A_2} \frac{\partial V}{\partial \alpha_2} + \frac{U}{A_1 A_2} \frac{\partial A_2}{\partial \alpha_1} + \frac{W}{R_2} \right) \\ \epsilon_\zeta &= \frac{\partial W}{\partial \zeta} \\ \gamma_{12} &= \frac{1}{1 + \frac{\zeta}{R_1}} \left(\frac{1}{A_1} \frac{\partial V}{\partial \alpha_1} - \frac{U}{A_1 A_2} \frac{\partial A_1}{\partial \alpha_2} \right) + \frac{1}{1 + \frac{\zeta}{R_2}} \left(\frac{1}{A_2} \frac{\partial U}{\partial \alpha_2} - \frac{V}{A_1 A_2} \frac{\partial A_2}{\partial \alpha_1} \right) \end{aligned} \quad (D-2)$$

$$\gamma_{1\zeta} = \frac{\partial U}{\partial \zeta} + \left(\frac{1}{A_1} \frac{\partial W}{\partial \alpha_1} - \frac{U}{R_1} \right) \cdot \frac{1}{\left(1 + \frac{\zeta}{R_1} \right)}$$

$$\gamma_{2\zeta} = \frac{\partial V}{\partial \zeta} + \frac{1}{1 + \frac{\zeta}{R_2}} \left(\frac{1}{A_2} \frac{\partial W}{\partial \alpha_2} - \frac{V}{R_2} \right)$$

where the functions U , V , and W represent the displacement components caused by straining of a material point originally at point $(\alpha_1, \alpha_2, \zeta)$ in the shell in the α_1 , α_2 , and ζ direction, respectively.

To incorporate the transverse shear deformation, the classical Kirchhoff-Love assumption must be abandoned. The material lines originally straight and normal to the midsurface of the shell remain straight but are no longer normal to the deformed midsurface (Figure 16). This implies that the transverse shear deformation is independent of the coordinate ζ . Hence, the shear rotation can be represented by some average value of the shear strain at midsurface. The displacement components of a point in the shell can be expressed, as a first approximation, by relationships of the form

$$\begin{aligned} U(\alpha_1, \alpha_2, \zeta) &= u(\alpha_1, \alpha_2) + \zeta \beta_1(\alpha_1, \alpha_2) \\ V(\alpha_1, \alpha_2, \zeta) &= v(\alpha_1, \alpha_2) + \zeta \beta_2(\alpha_1, \alpha_2) \\ W(\alpha_1, \alpha_2, \zeta) &= w(\alpha_1, \alpha_2) \end{aligned} \tag{D-3}$$

where u , v , and w are displacements of the point at midsurface, and β_1 and β_2 are rotations that represent changes of slope of the normal to the midsurface. It should be noted that terms u , v , w , β_1 and β_2 are functions of α_1 and α_2 only.

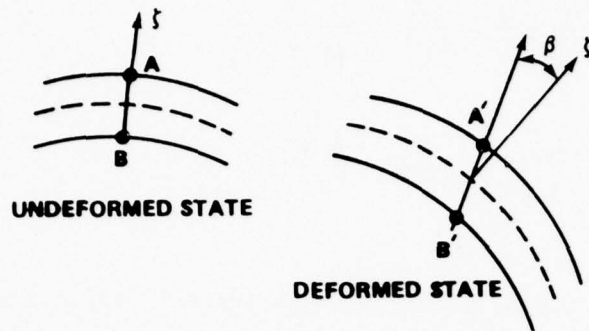


Figure 16. Transverse Shear Deformation.

Substituting Equations (D-3) into the strain-displacement relations Equation (D-2) and suppressing the terms $\frac{\zeta}{R_1}$ yield

$$\epsilon_1 = e_1 + \zeta \kappa_1$$

$$\epsilon_2 = e_2 + \zeta \kappa_2$$

$$\epsilon_\zeta = 0$$

$$\gamma_{12} = 2 e_{12} + \zeta (2 \kappa_{12}) \quad (D-4)$$

$$\gamma_{1\zeta} = \frac{1}{A_1} \frac{\partial w}{\partial \alpha_1} - \frac{u}{R_1} + \beta_1$$

$$\gamma_{2\zeta} = \frac{1}{A_2} \frac{\partial w}{\partial \alpha_2} - \frac{v}{R_2} + \beta_2$$

where

$$e_1 = \frac{1}{A_1} \frac{\partial u}{\partial \alpha_1} + \frac{v}{A_1 A_2} \frac{\partial A_1}{\partial \alpha_2} + \frac{w}{R_1} \quad (D-5)$$

$$e_2 = \frac{1}{A_2} \frac{\partial v}{\partial \alpha_2} + \frac{u}{A_1 A_2} \frac{\partial A_2}{\partial \alpha_1} + \frac{w}{R_2}$$

are the extensional strains at the midsurface of the shell,

$$\kappa_1 = \frac{1}{A_1} \frac{\partial \beta_1}{\partial \alpha_1} + \frac{\beta_2}{A_1 A_2} \frac{\partial A_1}{\partial \alpha_2} \quad (D-6)$$

$$\kappa_2 = \frac{1}{A_2} \frac{\partial \beta_2}{\partial \alpha_2} + \frac{\beta_1}{A_1 A_2} \frac{\partial A_2}{\partial \alpha_1}$$

are the changes in curvature of the midsurface in the directions of α_1 and α_2 , respectively, and

$$^2 e_{12} = \frac{1}{A_1} \frac{\partial v}{\partial \alpha_1} - \frac{u}{A_1 A_2} \frac{\partial A_1}{\partial \alpha_2} + \frac{1}{A_2} \frac{\partial u}{\partial \alpha_2} - \frac{v}{A_1 A_2} \frac{\partial A_2}{\partial \alpha_1} \quad (D-7)$$

$$^2 \kappa_{12} = \frac{1}{A_1} \frac{\partial \beta_2}{\partial \alpha_1} - \frac{\beta_1}{A_1 A_2} \frac{\partial A_1}{\partial \alpha_2} + \frac{1}{A_2} \frac{\partial \beta_1}{\partial \alpha_2} - \frac{\beta_2}{A_1 A_2} \frac{\partial A_2}{\partial \alpha_1}$$

represent the in-surface shear strain and twist of the midsurface, respectively.

STRESS-STRAIN RELATIONS

Assuming that the in-surface stresses can be represented by a state of generalized plane stress, the stress-strain relations for the shell space and for the orthotropic material can be written as

$$\sigma_1 = \frac{E_1}{1 - \nu_{12}\nu_{21}} \epsilon_1 + \frac{\nu_{21} E_2}{1 - \nu_{12}\nu_{21}} \epsilon_2$$

$$\sigma_2 = \frac{\nu_{12} E_1}{1 - \nu_{12}\nu_{21}} \epsilon_1 + \frac{E_2}{1 - \nu_{12}\nu_{21}} \epsilon_2$$

$$\tau_{12} = G_{12} \gamma_{12}$$

$$\tau_{1\xi} = G_{1\xi} \gamma_{1\xi} \quad (D-8)$$

$$\tau_{2\xi} = G_{2\xi} \gamma_{1\xi}$$

where E_1 , E_2 , G_{12} , $G_{1\xi}$, $G_{2\xi}$, ν_{12} , and ν_{21} are the elastic constants along the three coordinate directions [21].

Since the transverse shear strain has been assumed to be constant across the thickness, the corresponding shear stress is likewise constant and is directly proportional to the shear strain. However, from elementary strength of materials it is known that transverse shear stress is not constant across the thickness of a beam section. Therefore, the average shear strain, which may provide a good approximation to the shear rotation, does not necessarily provide an adequate representation of the shear stress distribution. Hence, a shear stress factor is used in conjunction with the transverse stress-strain Equation (D-8) as suggested by Naghdi [22], that is

$$\tau_{i\xi} = \frac{5}{6} G_{i\xi} \gamma_{i\xi} \quad i = 1, 2 \quad . \quad (D-9)$$

Substituting Equations (D-4) into Equations (D-8) and (D-9) and integrating across the thickness of the shell, the stress resultants and couples are obtained as follows:

$$N_1 = C_{11} e_1 + C_{12} e_2$$

$$N_2 = C_{21} e_1 + C_{22} e_2$$

$$N_{12} = 2G_{12} + e_{12}$$

$$M_1 = D_{11} \kappa_1 + D_{12} \kappa_2$$

$$(D-10) \quad M_2 = D_{21} \kappa_1 + D_{22} \kappa_2$$

$$M_{12} = \frac{G_{12} t^3}{12} (2 \kappa_{12})$$

$$Q_1 = \frac{5}{6} G_{1\zeta} t \gamma_{1\zeta}$$

$$Q_2 = \frac{5}{6} G_{2\zeta} t \gamma_{2\zeta}$$

where t is the thickness of the shell and

$$c_{11} = \frac{E_1 t}{1 - v_{12} v_{21}}$$

$$c_{22} = c_{11} \frac{E_2}{E_1}$$

$$D_{11} = \frac{E_1 t^3}{12(1 - v_{12} v_{21})} \quad (D-11)$$

$$D_{22} = D_{11} \frac{E_2}{E_1}$$

$$c_{12} = c_{21} = v_{12} c_{22} = v_{21} c_{11}$$

$$D_{12} = D_{21} = v_{12} D_{22} = v_{21} D_{11}$$

SHELLS OF REVOLUTION

The discussion will now be restricted to shells of revolution.

The midsurface of the shell is obtained by rotation of a plane curve.

This curve is called the meridian and its plane is the meridian plane.

The intersection of the surface with planes perpendicular to the axis of rotation are parallel circles and are called parallels. For shells

of revolution, the lines of principal curvature are its meridians and parallels [23].

A set of convected normal coordinates ϕ , θ , and ζ are used to describe the shells of revolution, where ϕ is the angle between the normal to the midsurface of the shell and the axis of revolution, θ is the angle describing the position of points of the corresponding parallel as shown in Figure 17. The radius of curvature of the meridian is R_1 . The second radius of curvature R_2 will always be the length of the intercept of the normal to the midsurface between the axis of the shell, i.e., \overline{AP} . This is because the normal from two adjacent points P and P' on the same parallel will always intersect on the axis of the shell.

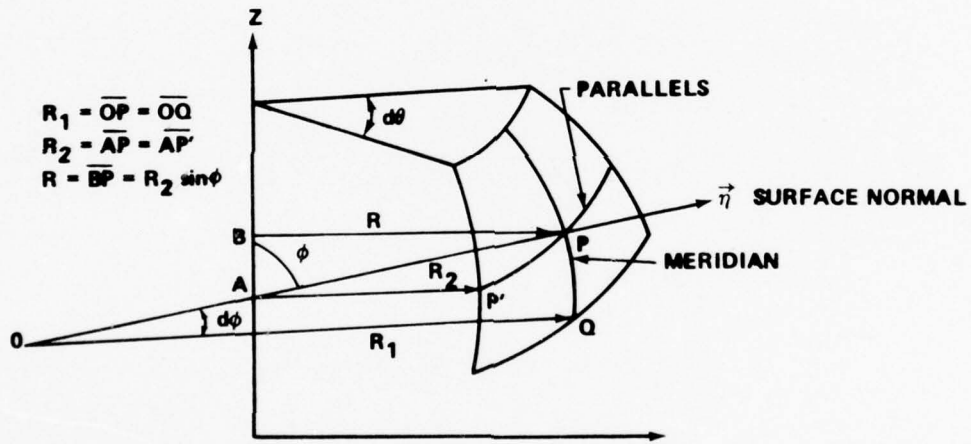


Figure 17. Shell Geometry.

The arc length of a line element in the shell space is given as

$$ds^2 = R_1^2 d\phi^2 + R_2^2 \sin^2 \phi d\theta^2 . \quad (D-12)$$

Associating α_1 with ϕ and α_2 with θ and comparing Equation (D-12) with Equation (D-1), the following is obtained:

$$A_1 = R_1$$

$$A_2 = R = R_2 \sin\phi . \quad (D-13)$$

Note that the term $\frac{\zeta}{R_i}$ in Equation (D-1) is small compared to unity for thin shells.

From Figure 18, by inspection, the following is obtained:

$$\frac{dR}{ds_1} = \cos\phi ,$$

or

$$\frac{dR}{d\phi} = R_1 \cos\phi . \quad (D-14)$$

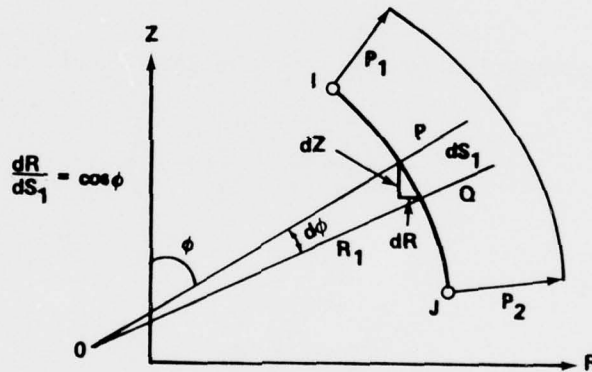


Figure 18. Shell Meridian.

AXISYMMETRIC LOADINGS

For shells of revolution with axisymmetric loadings, all geometric quantities are independent of θ . Consequently, all of the shell variables are independent of θ and, starting with the relationships between the strains and displacements Equations (D-4) through (D-7), the following is obtained:

$$e_1 = \frac{1}{R_1} \frac{du}{d\phi} + \frac{w}{R_1}$$

$$e_2 = \frac{1}{R} (u \cos\phi + w \sin\phi)$$

$$\kappa_1 = \frac{1}{R_1} \frac{d\beta_1}{d\phi} \quad (D-15)$$

$$\kappa_2 = \frac{\beta_1}{R} \cos\phi$$

$$\gamma_{1\xi} = \frac{1}{R_1} \frac{dw}{d\phi} - \frac{u}{R_1} + \beta_1 \quad .$$

Setting $\gamma_{1\xi}$ equal to some average shear strain as

$$\gamma_{1\xi} = -\gamma_1 \quad , \quad (D-16)$$

and substituting Equation (D-16) into the last Equation of (D-15) yields

$$\beta_1 = -\left(\frac{1}{R_1} \frac{dw}{d\phi} - \frac{u}{R_1} + \gamma_1\right) \quad . \quad (D-17)$$

Furthermore, let

$$\frac{1}{R_1} \frac{d}{d\phi} = \frac{d}{ds} \quad (D-18)$$

where s is measured along the meridional direction of the midsurface.

Substituting Equations (D-18) and (D-17) into Equation (D-15) the following is obtained:

$$e_1 = \frac{du}{ds} + \frac{w}{R_1}$$

$$e_2 = \frac{1}{R} (u \cos\phi + w \sin\phi)$$

$$\begin{aligned}\kappa_1 &= -\frac{d}{ds} \left(\frac{dw}{ds_1} - \frac{u}{R_1} + \gamma_1 \right) \\ \kappa_2 &= -\frac{\cos\phi}{R} \left(\frac{dw}{ds_1} - \frac{u}{R_1} + \gamma_1 \right) \\ \gamma_{1\xi} &= -\gamma_1\end{aligned}\quad (D-19)$$

The stress resultants and couples reduce from Equation (D-10) to the following set:

$$\begin{aligned}N_1 &= C_{11} e_1 + C_{12} e_2 \\ N_2 &= C_{21} e_1 + C_{22} e_2 \\ M_1 &= D_{11} \kappa_1 + D_{12} \kappa_2 \\ M_2 &= D_{21} \kappa_1 + D_{22} \kappa_2 \\ Q_1 &= \frac{5}{6} G_{1\xi} t \gamma_{1\xi}\end{aligned}\quad (D-20)$$

Appendix E

COMPUTER PROGRAM ORTHO2

The foregoing derivation was implemented in a finite element computer program. For convenience in reference, this program will be referred to as ORTHO2. The element stiffness matrix was formed by numerical integration. The nodal point coordinate and element connection array are generated automatically by the program. A shell of revolution is first divided into as many segments as necessary. Because each segment may be considered as a separate unit, different material properties as well as thickness and pressure can be ascribed to different segments. Each segment in turn may be subdivided into any number of shell elements. Normal pressure and thickness of the shell must be axisymmetric, but may be varied linearly along the meridional direction. The matrix equations are solved by the Cholesky decomposition process which stores only nonzero elements and therefore results in a significant saving of computing time. The program can be used to solve problems of thin, thick, and sandwich shells of revolution as well as multilayered, orthotropic shells such as a fiber reinforced composite. The program is limited to ten different materials and 50 nodes, but can be increased by increasing the dimension statement accordingly. This program requires about 32K core storage and three scratch files. A total of nine sets of input data is needed. The flow chart for ORTHO2 is shown in Figure 19.

An iteration procedure is used in the program. For the nonlinear effect, the load is applied in increments and the coordinates are updated.

This method was compared with that of using the relations in Equation (32a) and was found to give practically the same results. Much of the data is generated internally in the program.

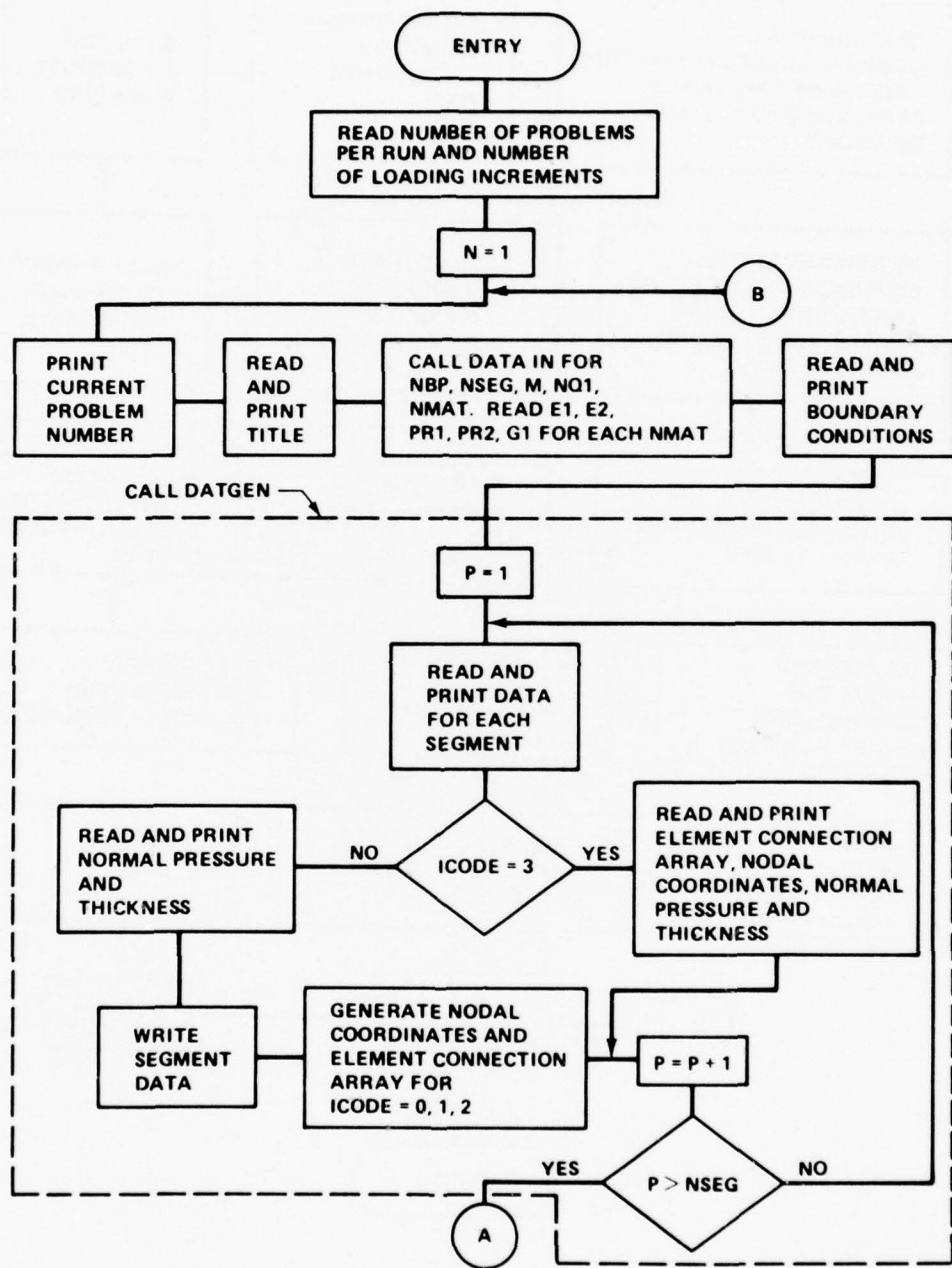


Figure 19. Flow Chart for ORTHO2.

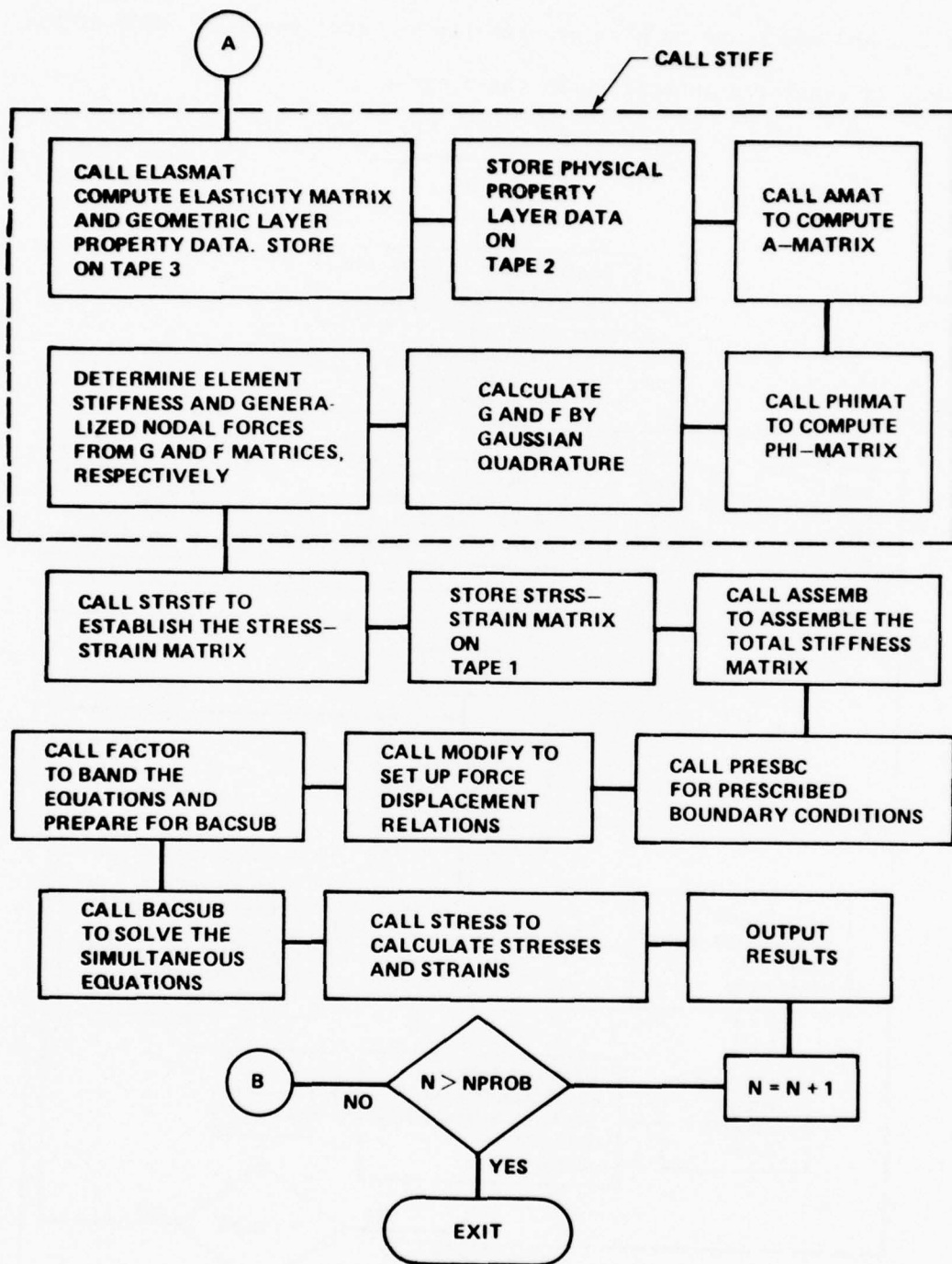


Figure 19. (Concluded).

DATA INPUT INSTRUCTIONS

1. Problem card; Load increment card (2I5):

Col. 1-5	Number of problems per run	(NPROB)
6-10	Number of load increments	(NINCR)

2. Title card (9A8):

Col. 1-72	Title to be printed with output	(TITLE)
-----------	---------------------------------	---------

3. Control card (5I5):

Col. 1-5	Number of boundary points	(NBP)
6-10	Number of segments	(NSEG)
11-15	Number of elements	(M)
16-20	Number of nodes	(NQ1)
21-25	Number of materials	(NMAT)

4. Material cards (7F10.0) one for each material:

Col. 1-10*	Young's modulus in meridional direction	(E1)
11-20*	Young's modulus in circumferential direction	(E2)
21-30	Poisson's ratio in meridional direction	(PR1)
31-40	Poisson's ratio in circumferential direction	(PR2)
41-50	Enter 0. for thin shell 1. for thick shell with $G = E/2(1+\nu)$ or shear modulus for thick or sandwich shell	(G1)

5. Boundary cards (5I5, 5X, 4F10.2) one for each boundary point:

Col. 1-5	Boundary node number	(I)
6-10	r-direction 0 free 1 fixed	(ID1)
11-15	z-direction 0 free 1 fixed	(ID2)
16-20	Normal rotation 0 free 1 fixed	(ID3)
21-25	Shear rotation 0 free 1 fixed	(ID4)
31-40	Prescribed r displacement	(UP)
41-50	Prescribed z displacement	(WP)
51-60	Prescribed rotation (angular displacement)	(THP)
61-70	Skewed boundary (angle)	(AL)

6. Segment cards (1X, 2I2, I5, 5 F10.2, 4I5) one for each segment:
- | | | |
|----------|--|----------|
| Col. 2-3 | 0 Conical segment (straight line) | (ICODE) |
| | 1 Spherical segment | |
| | 2 Elliptical segment | |
| | 3 Arbitrary curved segment | |
| 4-5 | Number of layers | (NLAYER) |
| 6-10 | 0 NLAYER is the same as the previous
segment | (LAYID) |
| | 1 New NLAYER for the segment
New layer data are required | |
| 11-20 | R-coordinate of the first node of the
segment | (R1) |
| 21-30 | Z-coordinate of the first node of the
segment | (Z1) |
| 31-40 | Total length of the segment if
ICODE = 0 | (A1) |
| | Total subtend angle of the segment if
ICODE = 1 | |
| | The difference in the R-coordinate of the
first and last node of the segment if
ICODE = 2 | |
| | Blank if ICODE = 3 | |
| 41-50 | Angle of slope between the straight line (A2)
segment and the r-axis if ICODE = 0 | |
| | Radius of the spherical segment if
ICODE = 1 | |
| | Major radius of the elliptic segment if
ICODE = 2 | |
| | Blank if ICODE = 3 | |
| 51-60 | Leave blank if ICODE = 0 | (A3) |
| | Phase angle ϕ between the normal to the
shell surface and the axis of revolution
if ICODE = 1 (to the first node of the
segment) | |
| | Minor radius of the elliptic segment if
ICODE = 2 | |
| | Blank if ICODE = 3 | |
| 61-65 | First element number of the segment | (M1) |
| 66-70 | Last element number of the segment | (M2) |
| 71-75 | First node number of the segment | (N1) |
| 76-80 | Last node number of the segment | (N2) |

7a. Pressure loading and thickness cards (8F10.2) one for each segment except ICODE = 3. (Replace 7a by 7b and 7c when ICODE = 3):

Col. 1-10	Normal pressure at the first node of the segment	(P1)
11-20	Normal pressure at the last node of the segment	(P2)
21-30	Thickness of the shell or thickness of the core layer of a sandwich shell at the first node of the segment	(T1)
31-40	Thickness of the shell or thickness of the core layer of a sandwich shell at the last node of the segment.	(T2)

Replace 7a by the following set if ICODE = 3.

7b. Element cards (5I10) one for each element:

Col. 1-10	Element number	(I)
11-20	Node I } element connection	(J)
21-30	Node J }	(K)
31-40	Number of layers	(MLAYER)
41-50	Layer identification code	(LID)

7c. Coordinate cards (I5, 5X, 2F10.2, 2F5.1, 4F10.2) one for each node:

Col. 1-5	Node number	(N3)
11-20	R-coordinate of the node	(R)
21-30	Z-coordinate of the node	(Z)
31-35	Angle between normal to the shell surface and the axis of symmetry	(PHA)
36-40	Meridian curvature of the shell	(KAPP)
41-50	Normal pressure at the node	(PP)
51-60	Thickness of the shell or thickness or the core layer of a sandwich shell	(TT)

8. Concentrated load cards (2I5, F10.2)** one for each load component plus one EOD card:

Col. 1-5	Node number	(I)
6-10	1 for r-component of the load 2 for z-component of the load 3 for moment loading	(NC1)
11-20	Magnitude of the loading. Positive if the direction of loading coincides with the positive direction of the coordinates	(V1)

9. Layer data (I5, 5X, 3F10.4) new set of data is required if there is a change in the number of layers:

Col. 1-5	Material type number	(MT1)
11-20	Distance from reference surface to top of layer at node I	(HI1)
21-30	Distance from reference surface to top of layer at node J	(HJ1)
31-40	Wrap angle	(ANGLE1)

*All Young's moduli must be scaled down by a factor of 10^6

**The last card of the set must contain a number greater than the total node number (End of Data Card).

A pressurized hemisphere-cylinder shell was chosen as an example for data preparation for the computer program. The shell as shown in Figure 20 is divided into four segments. There are two boundary points. With the boundary condition shown, there will be a boundary release at node No. 1 in the z-direction and at node No. 50 in the r-direction. The total subtend angles for segments 1 and 2 are 80° and 10° respectively (lines 7 and 9 of Figure 21). Note that the angle of slope between the straight line segments and the r-axis for segments 3 and 4 is -90° since the node numbers are increasing downward (see line 13 of Figure 21). A set of sample data cards for this structure is shown in Figure 21.

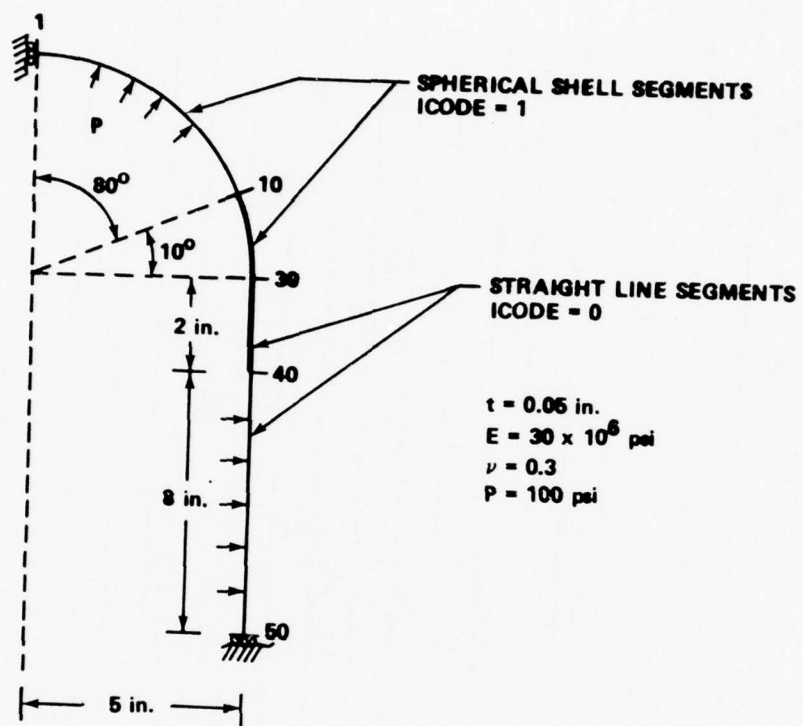


Figure 20. Hemisphere-Cylindrical Shell.

Col. No.	1	3	5	10	15	20	25	30	35	40	45	50	55	60	65	70	75	80
Card	1	1	10															
2 HEMISPHERE-CYLINDER SHELL																		
3	2	4	49	50	1													
4	30.	30.	.	.3	.													
5	1	1	0	1	1													
6	50	0	1	1	1													
7	1	1	1	0.	15.													
8	100.		100.		.05													
9	1	1																
10	100.		100.		.05													
11	0	1																
12	100.		100.		.05													
13	0	1																
14	100.		100.		.05													
15	1000																	
16	1		.025		.025													

Figure 21. Sample Data Cards.

```

PRUCKAV 5A1.. (INPUT)=65,(OUTPUT=65,TAPES=INPUT,TAPE6=OUTPUT,TAPE1,TAORTHO 2
TPE2,TAPE3)

C
C   VERSION 7
C   FINITE ELEMENT ANALYSIS OF AXISYMMETRIC LAMINATED SHELLS OF
C   REVOLUTION USING CURVED ELEMENT
C
C   GLOBAL COORDINATES + R-L
C
CCCCCCCC
      REAL   L,KAPPAL,KAPPB,KAPPAB
      REAL   RULL,NUCL
      COMMON  ELL(11C),NUCL(11C),NUCL(11C),NUCL(11C),GL(11C)
      *  ,FSAVE(10CC),XK(25C),FL(10CC)
      COMMON  CSFH1,SNFH1,CSFH2,SNFH2,KAPPAL,KAPPAB,SNPSI,CSPSI
      1  *  SNFH1,SNFH2,CSFH1,CSFH2
      COMMON  SIE,E),SE18),A1(b,8),G(8,8),GAA(8,8)
      1,LL1(10CC),R(25C),Z(25C),U(1000,8),F(1000)
      2,J(25C),K(25C),AL(25C),PH(250),KAPP(250)
      3,IPP(25C),C(5,5),SS(1C,8),SE(10,8)
      4,MAYER(5,5),PP(25C),TT(25C)
      5,LID(25C),LP(10CC)
      COMMON  ISF2(25)
      DIMENSION TITLE(5),L(4)
      READ(5,10) NPREL,NINCR
      10 FORMAT(215)
      DO 93C NPR=1,NPREL
      WRITE(6,B8.2)NPR
      8+01 FORMAT(1NC* PROBLEM NL. *,15//)
      READ(5,1111) TITLE
      WRITE(6,1112) TITLE
      1111 FORMAT(9A8)
      1112 FORMAT(1X,SAE,/,5X,*INPLI DATA*,*,//)
      FNINCR=NINCR
      FAC=1./FNINCR
      REWIND 3
      MAXDIF=C
      PI=3.141592653525
      R(1)=C.C

```

BEST AVAILABLE COPY

REST AVAILABLE COPY

```

9C19 FORMAT(//,* NCUAL FORCES *.* * NCUF CIR. NC. LOCAD*)
552 READ(5,553)1,NC1,V1
      WRITE(6,553)1,NC1,V1
553 FORMAT(215,F1C.2)
      IF(I>1)GOTO 56C
      K1=4*I-4+NC1
      F1(K1)=F1(K1)+V1*2.*PI.*R(I)
      IF(R(I).EQ.0.C.)F1(K1)=F1(K1)+V1
      GO TO 552
560 CONTINUE
      WRITE(6,38)
      WRITE(6,38)
38 FORMAT(/,1X,*ELEMENT NUMBER J K
      DO 3CC1 N1=1,M
      WRITE(6,361)N1,J(N1),K(N1),PLAYER(N1)
3001 CONTINUE
361 FORMAT(5I1C)
      WRITE(6,39)
      WRITE(6,39)
      39 FORMAT(/,1C,X,*ELEMENT LAYER MATERIAL HI
      DO 2CCC INCR=1,NINCR
      DO 13C II=1,N
      F(II)=C.
      DO 13C C JJ=1,NN
      130 U(II,JJ)=C.
      REWIND 1
      REWIND 2
      DO 43C II=1,M
      I=11
      T1=TT(J(1))
      TJ=TT(K(1))
      RI=R(J(1))
      RJ=R(K(1))
      ZI=Z(J(1))
      ZJ=Z(K(1))
      A=ZI-ZJ
      B=RJ-RI
      L=C.
      T3=A**2+B**2
      IF(T3.GT.C.)L=SQR(T3)
      IF(R1.EQ.0.C.)RI=1./1C.*#*16
      ORTHO 82
      ORTHO 83
      ORTHO 84
      ORTHO 85
      ORTHO 86
      ORTHO 87
      ORTHO 88
      ORTHO 89
      ORTHO 90
      ORTHO 91
      ORTHO 92
      ORTHO 93
      ORTHO 94
      ORTHO 95
      ORTHO 96
      ORTHO 97
      ORTHO 98
      ORTHO 99
      ANGLE*)
      ORTHO1C0
      ORTHO1C1
      ORTHO1C2
      ORTHO1C3
      ORTHO1C4
      ORTHO1C5
      ORTHO1C6
      ORTHO1C7
      ORTHO1C8
      ORTHO1C9
      ORTHO110
      ORTHO111
      ORTHO112
      ORTHO113
      ORTHO114
      ORTHO115
      ORTHO116
      ORTHO117
      ORTHO118
      ORTHO119
      ORTHO120
      ORTHO121

```

BEST AVAILABLE COPY

```

IF(RJ.EQ.C)RJ=1./LC.*.**16
FNJ=XX(11)
CALL STIFF(11,PI.RI,A,B,L,ZI,RJ,ZJ,I.NCR,FNJ)
CALL STRSTF(11,RI,RJ,TJ)
WRITE(11),SSS,R1,R2,T,SE
CALL ASSEM(11)

430 CONTINUE
DO 440 I2=1,N
440 F(I2)=(F(I2)+T(11)*FAC
CALL PRESBC(N,NN,DP,L,LL1)
DO 1CCC 11=1,NC1
IF( AL(11).EQ.C.) GC TC 1CC0
K4=4*(11-1)+1
AL1=AL(11)*PI/18C.
ALF = TAN(11)
CALL MODIFY(F,L,NN,K4,ALF)
1000 CONTINUE
CALL FACTOR(N,Nb,L,LL1)
CALL BACSLH(N,Nb,L,LL1,F)
DO 810 I1=1,N
810 FSAVE(11)=SAVE(11)+F(11)
CALL STRESSIM,INCR,NINCR)
IF(INCR.EQ.NINCR) WRITE(16,800)
800 FORMAT(//,5X,*NODAL DISPLACEMENT*,*/
1* NODE*,12X,*R-DIRECTION*,7X,*Z-DIRECTION*,7X,
2*R UPDATED*,7X*2 UPDATED*,5X,
2*NORMAL ROTATION*,5X,* SHEAR ROTATION*/)
WRITE(6,900) INCR
900 FORMAT(1X,7HINCR = ,13)
DU S27 11=1,NC1
K1=4*11-4
DO 928 JJ=1,4
928 W(JJ)=FSAVE(K1+JJ)
UC=PP(11)
MC=TT(11)
R(11)=R(11)+F(K1+1)
Z(11)=Z(11)+F(K1+2)
PH(11)=PHA(11)-F(K1+3)*180./PI
IF(INCR.EQ.NINCR)
1WRITE(6,S29) 11,Q(1),Q(2),R(11),Z(11),C(3),Q(4)

```

BEST AVAILABLE COPY

```

927 CONTINUE          ORTHO162
2000 CONTINUE          ORTHO163
929 FORMAT(1X,*,LPtE,7) ORTHO164
930 CONTINUE          ORTHO165
9999 CALL EXIT        ORTHO166
END                  ORTHO167
SUBROUTINE DATAIN(NBP,NSEG,M,NC1)      ORTHO168
REAL    NUCL,NUCL      ORTHO169
COMMON   EL(1C),EC(10),NUCL(10),NUCL(10),GL(10)
* ,FSAVE(1CCC),X*(25C),FL(1CC0)
C
C NBP, NUMBER OF TOTAL BOUNDARY PLINTS      ORTHO170
C NSEG, NUMBER OF TOTAL SEGMENTS            ORTHO171
C M, NUMBER OF TOTAL ELEMENTS              ORTHO172
C NO1, NUMBER OF TOTAL NODES               ORTHO173
C NMAT, NUMBER OF TOTAL MATERIALS          ORTHO174
C
C READ(5,1C) NBP,NSEG,M,NC1,NMAT          ORTHO175
10 FORMAT(5I5)           ORTHO176
      WRITE(6,11) NBP,NSEG,M,NC1,NMAT      ORTHO177
11 FORMAT(IX,*NUMBER OF BOUNDARY POINTS=** 15//,
      *NUMBER OF SEGMENTS=** 15///,
      1           *NUMBER OF ELEMENTS=** 15///,
      2           *NUMBER OF NODES=** 15///,
      3           *NUMBER OF MATERIALS=** 15///,
      4           )
C
C ONE SET OF MATERIAL DATA FOR EACH MATERIAL      ORTHO178
C E1,E2 YOUNG-S MODULUS          ORTHO179
C PR1,PR2 POISSON'S RATIOS       ORTHO180
C G1,SHEAR MODULUS             ORTHO181
C G1=1, SHEAR MODULUS IS SET EQUAL TO E/2(1+V) ORTHO182
C G1=0., TRANSVERSE SHEAR EFFECT IS SUPPRESSED ORTHO183
C
C WRITE(6,12)                 ORTHO184
12 FORMAT(1X,*MATERIAL   EL      ORTHO185
      1           GL *)                   NC1      ORTHO186
                                         NUCL      ORTHO187
                                         NUCL      ORTHO188
                                         NUCL      ORTHO189
                                         NUCL      ORTHO190
                                         NUCL      ORTHO191
                                         NUCL      ORTHO192
                                         NUCL      ORTHO193
                                         NUCL      ORTHO194
                                         NUCL      ORTHO195
                                         NUCL      ORTHO196
                                         NUCL      ORTHO197
                                         NUCL      ORTHO198
                                         NUCL      ORTHO199
                                         NUCL      ORTHO200
                                         NUCL      ORTHO201

```

BEST AVAILABLE COPY

```

DO 3C L11=1,NMAT
READ(5,21) E1,E2,PRI,PR2,G1
21 FORMAT(7F1C,C)
E1=E1*1C.**E
E2=E2*1C.**E
IF(G1.EQ.1.C) G1=E1/(2.*(1.+PRI))
WRITE(6,22) L11,E1,E2,PRI,PR2,G1
22 FORMAT(1X,14.7E14.3)
IF(G1.EQ.C) G1=1C.**5C
EL(L11)=E1
EC(L11)=E2
NULC(L11)=PRI
NUCL(L11)=PR2
GL(L11)=G1
30 CONTINUE
IF(G1.GT.1C.**3C) WRITE(6,20)
20 FORMAT(1X,/,# TRANVERSE SHEAR EFFECT IS NEGLECTED FOR THIS PROB.*ORTHO218
1.,/)
RETURN
END
SUBROUTINE DATGEN(NSEG, N)
REAL KAPP
COMMON ISFC1 (23CC)
COMMON ISFC (12)
COMMON S(E,E)*GE(8)*AA(8,8)*G(8,8)*GAA(8,8)
1.LL1(1CCC),R(25C),Z(25C),L(1000, 8),F(1000)
2.J(25C),K(25C),AL(250),PHA(250),KAPP(250)
3 * IPP(25C),C(5,5),S(10,8),SE(10,8)
4*MLAYER(25C),PP(25C),TT(25C)
5,LID(25C),UP(1CCC)
PI=3.141592653589
DO 2001 LID(L11)=C
2001 LID(L11)=C
C
C ICODE=C, STRAIGHT LINE SEGMENT, A1=TCTAL LENGTH, A2=SLOPE ANGLE
C ICODE=1, CIRCULAR SEGMENT, A1=TOTAL SUBTEND ANGLE, A2=RADIUS, A3=PHASE
C ANGLE.
C ICODE=2 ELLIPTIC SEGMENT A1=HORIZONTAL PROJECTION OF THE SEGMENT
C LENGTH, A2=MAJOR AXIS, A3=MINOR AXIS
C
ORTHO2C2
ORTHO2C3
ORTHO2C4
ORTHO2C5
ORTHO2C6
ORTHO2C7
ORTHO2C8
ORTHO2C9
ORTHO2C10
ORTHO211
ORTHO212
ORTHO213
ORTHO214
ORTHO215
ORTHO216
ORTHO217
ORTHO218
ORTHO219
ORTHO220
ORTHO221
ORTHO222
ORTHO223
ORTHO224
ORTHO225
ORTHO226
ORTHO227
ORTHO228
ORTHO229
ORTHO230
ORTHO231
ORTHO232
ORTHO233
ORTHO234
ORTHO235
ORTHO236
ORTHO237
ORTHO238
ORTHO239
ORTHO240
ORTHO241

```

BEST AVAILABLE COPY

```

C ICODE=3 * ARBITRARY CURVED SEGMENT
C NLAYER = NUMBER OF LAYERS
C LAYERID=C LAYER IS THE SAME AS THE PREVIOUS SEGMENT
C LAYERID=1 NEW LAYER FOR THE SEGMENT NEW LAYER DATA IS REQUIRED
C R1,Z1 COORDINATES OF THE FIRST NODE OF THE FIRST SEGMENT
C N1,N2, THE FIRST AND LAST NODE NO. OF SEGMENT
C M1,M2 THE FIRST AND LAST ELEMENT NO. OF SEGMENT
C

DO 1260 IJ=1,NSEG
  READ(5,190) ICODE,NAYER,LAYERID,R1,Z1,A1,A2,A3,M1,M2,N1,N2
  WRITE(6,190) ICODE,NAYER,LAYERID,R1,Z1,A1,A2,A3,M1,M2,N1,N2
190  FORMAT(IX,2I2,15,2F10.2,4I5)
100  FORMAT(7,3I5,5F10.2,4I5)
    IF(R1.EQ.C.C.AND.Z1.EQ.C.C) GO TO 4000
    GO TO 4C1
4000 CONTINUE
    R1 = R(N1)
    Z1 = Z(N1)
4001 CONTINUE
    IP=ICODE+1
    IF(IP.NE.4) GO TO 371
    WRITE(6,31) IJ
    DO 373 IK=M1,M2
    IPP(IK)=IP
    READ(5,361) I,J(I),K(I),PLAYER(I),LIC(I)
373 CONTINUE
361 FORMAT(5I1C)
    MEL=M2-M1+1
    YP1=MEL+1
    DO 8C IJK=1,NPL
      READ(5,194)N3,R(N3),Z(N3),PHA(N3),KAPF(N3),PP(N3),TT(N3)
      WRITE(6,195) N3,R(N3),Z(N3),AL(N3),PP(N3),TT(N3),PHA(N3)
80  CONTINUE
194  FORMAT(15,5X,2F10.2,2F5.1,4F10.2)
    GO TO 1260
C
C P1=NORMAL PRESSURE AT NODE I
C P2==NORMAL PRESSURE AT NODE J

```

BEST AVAILABLE COPY

```

C T1=TOTAL THICKNESS AT NODE I
C T2=TOTAL THICKNESS AT NODE J
C
C 371 CONTINUE
    READ(5,19) P1,P2,T1,T2
    WRITE(6,19) P1,P2,T1,T2
19   FORMAT(8F1C.2)
    DELP=(P2-P1)/(N2-N1)
    DELT=(T2-T1)/(N2-N1)
    DELX=A1/(N2-N1)
    SLOPE=A2*PI/1EC.
    WRITE(6,31) IJ
31   FORMAT(/,1X,* SEGMENT N1.*15.,*, NODE
          11          PHA*)
    DO 375 IK=M1,M2
    IPP(IK)=IP
    I=IK
    J(I)=IK
    K(I)=IK+1
    MAYER(I)=NAYER
    IF(IK.EQ.M1) LIU(I)=LAYID
375 CONTINUE
376 CONTINUE
    DO 26C I1=N1,N2
    IF(IJ.NE.1.AND.I1.EQ.N1) SU TU 192
    I#I1-N1+1
    PP(I1)=P1+DELP*(I-1)
    TT(I1)=T1+DELT*(I-1)
    GO TU (263,261,262,260),IP
263 CONTINUE
    DR=DELX*COS(SLCPE)*(I-1)
    DZ=DELX*SIN(SLCPE)*(I-1)
    RI11=R1+DK
    Z(I1)=Z1+DZ
    PHA(I1)=-A2
    KAPP(I1)=0.
    GO TU 152
261 CONTINUE
    RAD=A2

```

BEST AVAILABLE COPY

```

C ANG1=A3*PI/18C.
C ANG=DELX*(PI/18C.)*(1-1)+A3*PI/180.
C DZ=RAD*SIN(ANG)-RAU*SIN(ANG)
C DR=RAD*COS(ANG)-RAD*COS(ANG)
C DR=RAD*SIN(ANG)-RAD*SIN(ANG)
C DZ=RAD*COS(ANG)-RAD*COS(ANG)
R(11)=K1+DR
Z(11)=Z1+DZ
PHAI(11)=A3*DELX*(1-1)
KAPP(11)=1./RAD
GO TO 192
262 CONTINUE
DR=DELX*(1-1)
R(11)=R1+DR
Z(11)=(A2*A2*A3*A3-A3*A3*R(11)*R(11))/(A2*A2)*.5
RR=(A2*.4*R(11)**2+A3**4*Z(11)**2)**.5
RR1=RR*.3/(A2*.4*A3**4)
RR2=RR/(A3**2)
SNPHI=R(11)/RR**2
PHAI(11)=ASIN(SNPHI)*18C./PI
KAPP(11)=1./RK1
192 WRITE(6,195) 11, H(11), Z(11), AL(11), PF(11), TT(11), PHA(11)
199 FORMAT(1X,14,5X,7F1C.3)
260 CONTINUE
1260 CONTINUE
RETURN
END
SUBROUTINE ASSEMB(11)
REAL KAPP
COMMON ISFL1 (23CC)
COMMON ISFLC(12)
COMMON ST E, GT (8), AA (8,8), G (8,8), F (8,8)
1,LL1(1CCCC), R(250), L(25C), U(1000, 8), F(1000)
2, J(25C), K(25C), AL(25C), PHA(250), KAPP(250)
3, IPP(25C), C(5,5), SS(10,8), SE(10,8)
4, MLAYER(25C), PP(25C), TT(250)
5, LIU(250), LP(1CCCC)
DIMENSION KK(E)
KK(4)=4.*J(11)
KK(8)=4.*K(11)

```

BEST AVAILABLE COPY

```

KK(3)=KK(4)-1
KK(2)=KK(3)-1
KK(1)=KK(2)-1
KK(7)=KK(8)-1
KK(6)=KK(7)-1
KK(5)=KK(6)-1
DO 400 M=1,E
  LI=K(M)
  DO 400 N=1,E
    IF(K(N)*LI,LI) GO TO 400
    JJ=K(N)-LI+1
    U(LI,JJ)=U(LI,JJ)+S(M,N)
 400 CONTINUE
  RETURN
END
SUBROUTINE MODIFY(F,L,NN,K4,ALF)
DIMENSION F(1),L(1CCC,8)
F(K4)=F(K4)+ALF*F(K4+1)
F(K4+1)=C.
U(K4,1)=U(K4,1)+ALF*(L((K4+1,1)+1,)+2.*U(K4,2))
U(K4,2)=-ALF
U(K4+1,1)=I.
DO 29 N1=3,NN
 29 U(K4,N1)=U(K4,N1)+ALF*L((K4+1,NN+1)
  DO 28 N1=2,NN
    28 U(K4+1,N1) =C.
K5=K4-1
DO 34 N1=1,K5
  N11=N1+1
  N12=N1+2
  IF (N11.GT.NN) GC TC 34
  IF (N12.GT.NN) GC TC 34
  U(K4-N1,N1+1)=L((K4-N1,NN+1))+ALF*U((K4-N1,NN+2))
  U(K4-N1,N1+2)=C.
 34 CONTINUE
  RETURN
END
SUBROUTINE PRESBC(N,NN,DP,L,F,LL1)
DIMENSION DP(1),F(1),U(1CCC,8),LL1(1)
DO 200 N1=1,N
 200

```

BEST AVAILABLE COPY

```

IF(LL1(N1).NE.1) GO TO 200
DO 100 M1=2,NN
K1=N1-M1+1
IF(K1.LE.C) GO TO 5C
F(K1)=F(K1)-L(K1,M1)*DP(N1)
U(N1,M1)=C.
50 K1=N1+M1-1
IF(K1.GT.N) GO TO 1CC
F(K1)=F(K1)-L(N1,M1)*UP(N1)
U(N1,M1)=C.
100 CONTINUE
U(N1,1)=1.
F(N1)=DP(N1)
200 CONTINUE
RETURN
END
SUBROUTINE FACTOR(N,NBAND,L,LL1)
DIMENSION L((1CCC,8),LL1(1))
DO 16C I=1,N
IF(LL1(I).EQ.1) GO TO 16C
S1=0.
NW1=MAXC(1,I-NBAND)
KK=I-1
IF(KK.LT.NB1) GO TO 51
DO 5C K=NW1,KK
IF(LL1(K).EQ.1) GO TO 5C
40 S1=S1+U(K,I-K+1)**2*L(K,1)
50 CONTINUE
51 U(I,1)=U(I,1)-S1
NW2=MINC(N,I+NBAND)
JJ=I+1
IF(JJ.GT.NB1) GO TO 160
DO 15C J=JJ,NB2
IF(LL1(J).EQ.1) GO TO 15C
90 S2=0.
NW1=MAXC(1,J-NBAND)
K1=I-1
IF(K1.LT.NB1) GO TO 141
DO 14C K=NW1,K1
IF(LL1(K).EQ.1) GO TO 140

```

BEST AVAILABLE COPY

```

130 S2=S2+U(K,I-K+1)*L(K,1)*L(K,J-K+1)
ORTHO442
140 CONTINUE
ORTHO443
141 U(I,J-I+1)=(L(I,J-I+1)-S2)/L(I,J)
ORTHO444
150 CONTINUE
ORTHO445
160 CONTINUE
ORTHO446
RETURN
ORTHO447
END
SUBROUTINE BACSLB(N,NBAND,L,LL1,F)
DIMENSION L(1:CC,E),LL1(I),F(I)
DO 6C I=1,N
IF(LL1(I).EQ.1) GC IC 6C
S1=0.
NW1= MAXC(1,1-NBAND)
KK=I-1
IF(IKK.LT.NW1)GC IC 51
DO 5C K1=NW1,KK
IF(LL1(K1).EQ.1) GU IC 5C
40 S1=S1+U(K1,I-K1+1)*F(K1)
5C CONTINUE
51 F(I)=F(I)-S1
6C CONTINUE
C BACKWARD SUBSTITUTION
DO 11C I=1,N
I=N+1-1
IF(LL1(I).EQ.1) GC IC 11C
S1=C.
NW2= MINC(N,1+NBAND)
J1=I+1
IF((J1.GT.NW2))GC IC 1C1
DO 1CC JJ= J1,NW2
IF(LL1(JJ).EQ.1) GU IC 1C0
S1=S1+U(I,1)*L(I,JJ-1+1)*F(JJ)
100 CONTINUE
101 CONTINUE
F(I)=(F(I)-S1)/L(I,J)
110 CONTINUE
RETURN
END
SUBROUTINE STIFF(I,P1,R1,A,B,L,Z1,RJ,ZJ,INCR,FN,J)
REAL L,KAPPAL,KAPPB,KAPPAI,KAPPBJ
ORTHO448
ORTHO449
ORTHO450
ORTHO451
ORTHO452
ORTHO453
ORTHO454
ORTHO455
ORTHO456
ORTHO457
ORTHO458
ORTHO459
ORTHO460
ORTHO461
ORTHO462
ORTHO463
ORTHO464
ORTHO465
ORTHO466
ORTHO467
ORTHO468
ORTHO469
ORTHO470
ORTHO471
ORTHO472
ORTHO473
ORTHO474
ORTHO475
ORTHO476
ORTHO477
ORTHO478
ORTHO479
ORTHO480
ORTHO481

```

BEST AVAILABLE COPY

```

REAL NLLC,NLCL
DIMENSION M(11C),H1(1C),HJ(1C),ANGLE1(10),
COMMON EL(10),EC(10),NUCL(10),NULC(10),GL(10)
* .FSAVE(1CCC),XK(25C),F1(1000)
COMMON CSPHI,SNPHI,CSPHJ,SNPHJ,KAPPAL,KAPPAJ,SNPSI,CSPSI
1 SNBTI,Snb1J,Csb1I,Csb1J
COMMON S(8,E),GE(8),AA(8,8),G(8,8),GAA(8,8),
1.LL1(1CCC),F(250),Z(25C),U(1000,8),F(1000)
2.J(25C),K(25C),ALP(25C),PHA(250),KAPF(250)
3.IPP(25C),C(5,5),SS(10,8),SE(10,8)
4,MLAYER(25C),PP(25C),TT(25C)
5.LID(25C),UPI(1CCC)
COMMON /SET12/,AUT(2,2),AL(2,2),DSIARC(2,2),DISTARL(2,2),
1DSTAR(12,2),DU(12,2),UL(2,2),D1(2,2),L2(2,2),GEARC,GBARL
DIMENSION XI(2),AI(2),PHI(15,8),
1.PHPI(8,8),PHIPA(8,8),SI(8,8)
DATA XI/-5773C2692,577302692/
DATA AI/1..1./
C***** INITIALIZATION
DO 1 N1=1,E
FP(N1)=C.
FP(A(N1))=C.
DO 1 N2=1,E
C(N1,N2)=C.
1 GAA(N1,N2)=C.
DO 2 N1=1,5
DO 2 N2=1,E
2 DD(N1,N2)=C.
DO 3 N1=1,5
DO 3 N2=1,E
3 C(N1,N3)=C.
DEL P=PP(K(1))-PP(J(1))
P=PP(J(1))
T1=TT(J(1))
TJ=TT(K(1))
T=(T1+TJ)/2.
KP1=J(1)
K1=4*KP1-4
SNPSI=E/L
CSPSI=A/L
ORTHO482
ORTHO483
ORTHO484
ORTHO485
ORTHO486
ORTHO487
ORTHO488
ORTHO489
ORTHO490
ORTHO491
ORTHO492
ORTHO493
ORTHO494
ORTHO495
ORTHO496
ORTHO497
ORTHO498
ORTHO499
ORTHO500
ORTHO501
ORTHO502
ORTHO503
ORTHO504
ORTHO505
ORTHO506
ORTHO507
ORTHO508
ORTHO509
ORTHO510
ORTHO511
ORTHO512
ORTHO513
ORTHO514
ORTHO515
ORTHO516
ORTHO517
ORTHO518
ORTHO519
ORTHO520
ORTHO521

```

BEST AVAILABLE COPY

```

IF(INCR.NE.1) GO TO 613
IP=IP(I)
GU TU (2C1C+3C1C)+IF
CSPHI=SNPSI
SNPHI=CSPSI
CSPHJ=SNPSI
SYPHJ=CSPSI
KAPPAl=C.
KAPPAJ=C.
GU TU 41CC
3C10 CONTINUE
PHII=PHA(J(I))*PI/18.C.
PHIJ=PHA(K(I))*PI/18.C.
CSPHI=CSPIPHII
SNPHI=SIN(PHI)
CSPHJ=COS(PHI)
SNPHJ=SIN(PHI)
KAPPAl=KAPP(U(I))
KAPPAJ=KAPP(K(I))
41C0 CONTINUE
NLAYER=MAYER(I)
LIID=LID(I)
HN1=-T/2.
HNJ=-T/2.
DU 6C5 N1=1,2
DO 6C5 N2=1,2
AD(N1,N2)=C.
AL(N1,N2)=C.
DSTARO(N1,N2)=C.
DSTARL(N1,N2)=C.
DSTAR1(N1,N2)=C.
DO(N1,N2)=C.
DL(N1,N2)=C.
D1(N1,N2)=C.
D2(N1,N2)=C.
605 CONTINUE
GBARU=C.
GBARL=C.
ORTH0522
ORTH0523
ORTH0524
ORTH0525
ORTH0526
ORTH0527
ORTH0528
ORTH0529
ORTH0530
ORTH0531
ORTH0532
ORTH0533
ORTH0534
ORTH0535
ORTH0536
ORTH0537
ORTH0538
ORTH0539
ORTH0540
ORTH0541
ORTH0542
ORTH0543
ORTH0544
ORTH0545
ORTH0546
ORTH0547
ORTH0548
ORTH0549
ORTH0550
ORTH0551
ORTH0552
ORTH0553
ORTH0554
ORTH0555
ORTH0556
ORTH0557
ORTH0558
ORTH0559
ORTH0560
ORTH0561

```

BEST AVAILABLE COPY

```

C LAYER DATA
C NEW SET OF DATA IS REQUIRED IF THERE IS A CHANGE IN NUMBER OF LAYER
C MT1=MATERIAL TYPE NUMBER
C H11=DISTANCE FROM REFERENCE SURFACE TC TCF CF LAYER AT NODE I
C HJ1=DISTANCE FROM REFERENCE SURFACE TC TCF CF LAYER AT NODE J
C ANGLE1=WRAP ANGLE
C
C
      DD 61C 1JK=1,NLAYER
      IF(L1D1.NE.1) GO TO 604
      READ(5,611) M11(IJK),H11(IJK),HJ1(IJK),ANGLE1(IJK)
      WRITE(6,612) 1,IJK,M11(IJK),H11(IJK),HJ1(IJK),ANGLE1(IJK)
      604  CQN1ANGLE
      M11=M11(IJK)
      H1=H1(IJK)
      HJ=HJ1(IJK)
      ANGLE=ANGLE1(IJK)
      CALL ELASMA(M1,I,H1,HNI,ANGLE,IJK,HJ,HNJ,TI,TJ)
      HNI=H1
      HNJ=HJ
      610  CONTINUE
      611  FORMAT(15,5X,2F10.4)
      612  FORMAT(1X,2I1C,3F1C.4)
      GSTAR0=TJ/GBARU
      GSTARL=TJ/GBARL
      WRITE(2) AD,AL,DSTAR0,DSTARL,DSTAR1,CC,DL,C1,C2,GSTAR0,GSTARL
      GO TO 614
      613  CONTINUE
      READ(2) AD,AL,DSTAR0,DSTARL,DSTAR1,CC,DL,C1,C2,GSTAR0,GSTARL
      PHI1=PHA(J(1))*PI/18C.
      PHIJ=PHA(K(1))*PI/18C.
      THETAI=(PHI1-PHIJ)/2.
      KAPPAl=2.* SIN(THETAI)/L
      KAPPAJ=KAPPAl
      CSPHI=CO(S(PHI1))
      SNPHI=SI(N(PHI1))
      CSPHJ=CO(S(PHIJ))
      SNPHJ=SI(N(PHIJ))
      614  CONTINUE
      SNHTI=CSPHI*CSPSI-SNPHI*SNPSI
      ORTHO562
      ORTHO563
      ORTHO564
      ORTHO565
      ORTHO566
      ORTHO567
      ORTHO568
      ORTHO569
      ORTHO570
      ORTHO571
      ORTHO572
      ORTHO573
      ORTHO574
      ORTHO575
      ORTHO576
      ORTHO577
      ORTHO578
      ORTHO579
      ORTHO580
      ORTHO581
      ORTHO582
      ORTHO583
      ORTHO584
      ORTHO585
      ORTHO586
      ORTHO587
      ORTHO588
      ORTHO589
      ORTHO590
      ORTHO591
      ORTHO592
      ORTHO593
      ORTHO594
      ORTHO595
      ORTHO596
      ORTHO597
      ORTHO598
      ORTHO599
      ORTHO600
      ORTHO601

```

BEST AVAILABLE COPY

AD-A046 401

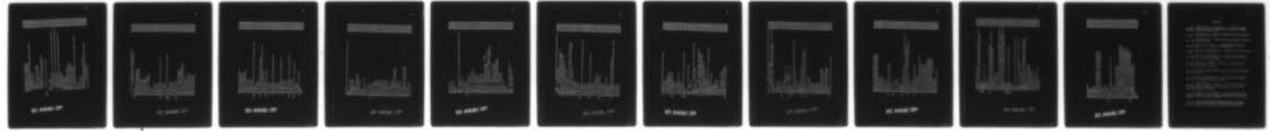
ARMY MISSILE RESEARCH AND DEVELOPMENT COMMAND REDSTO--ETC F/G 20/11
NONLINEAR ANALYSIS OF ORTHOTROPIC, LAMINATED SHELLS OF REVOLUTI--ETC(U)
AUG 77 C M ELDRIDGE

UNCLASSIFIED

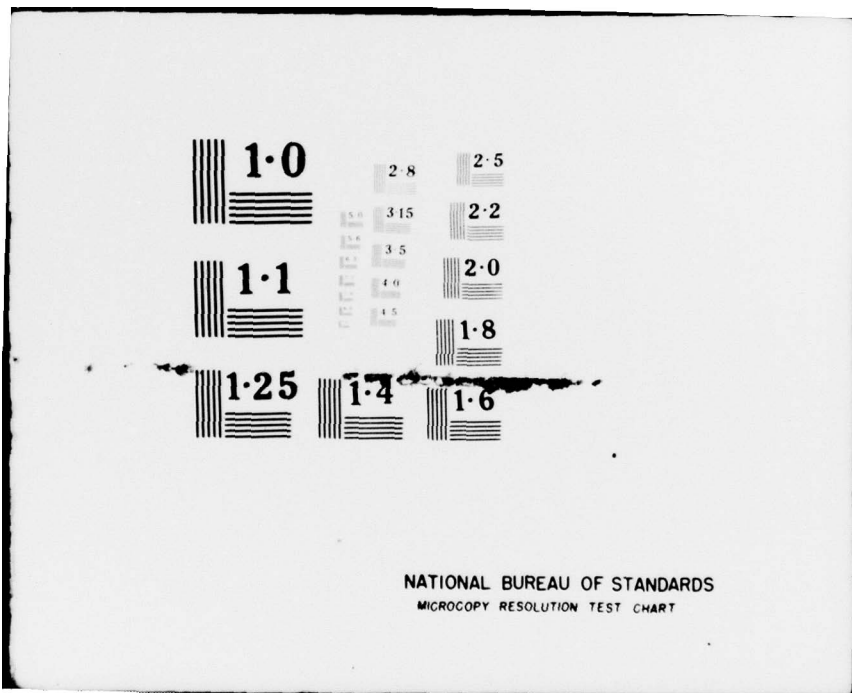
DRDMI-TL-77-9

NL

2 OF 2
ADA
046401



END
DATE
FILMED
12-77
DDC



```

SNBTJ=CSPHJ*CSPSI-SNPHJ*SNSPI
CSBTI=SNPHI*CSPSI+CSPHI*SNSPI
CSBTJ=SNPHJ*CSPSI+CSPHI*SNSPI
CALL AMAT(IA,SNPSI,CSPSI,L,SNBTJ,CSPBTJ,CSBTJ)
ETAPJ=SNBTJ/CSPBTJ
ETAPJ=SNBTJ/CSPBTJ
B1=ETAPJ
ETAPPJ=-KAPPAL/(CSE TI **3)
ETAPPJ=-KAPPAJ/(CSBTJ**3)
B2=B1+ETAPPJ*L/2.
B3=ETAPPJ*L/2.-4.*TAPJ-3.*B1-2.*B2
B4=3.*ETAPPJ+2.*B1+B2-L*ETAPPJ/2.

C***** GAUSSIAN QUADRATURE INTEGRATION
C
DO 4 NI=1,2
Y=L*(1.+XI(NI))/2.
ETA=B1*Y+(B2-B1)*Y**2/L+(B3-B2)*Y**3/L**2+(B4-B3)*Y**4/L***3
1 -B4*Y**5/L**4
ETAP=B1+Z.* (B2-B1)*Y/L+3.* (B3-B2)*Y/Y/L/L+4.* (B4-B3)*Y**3/L***3
1 -5.*B4*Y**4/L**4
ETAPP=2.* (B2-B1)/L+6.* (B3-B2)*Y/L**2+12.* (B4-B3)*Y/Y/L**3
1 -2C.*B4*Y**3/L**4
BETA=ATAN(ETAP)
CSBT=CD(SIBETA)
SNBT=SIN(BETA)
KAPPAL=-ETAPP*(CSPBT**3)
CSPHIX=SNBT*CSPSI+CSPBT*SNSPI
SNPHJX=CSPBT*CSPSI-SNBT*SNSPI
RR=R1+(Y*SNPSI+E1A*CSPSI)
XMUL=A1(NI)*RR/CSPBT*C.S*L
CALL PHIMAT(PHI,CSPBT,SNBT,SNPSI,CSPSI,RR,KAPPAL,Y,CSPHIX)
X=1.-Y/L
Z=Y/L
DO 3CC NI=1,2
DO 3CC NJ=1,2
C(NI,NJ)=X*AC(NI,NJ)+ZZ*AL(NI,NJ)
C(NI,NJ+2)=X*X*USTARU(NI,NJ)+Z*Z*CSTARL(NI,NJ)
1 +X*Z*Z*DSTAR1(NI,NJ)
C(NI+2,NJ)= C(NI,NJ+2)

```

BEST AVAILABLE COPY

```

C(NI+2,NJ+2)=X*X*X*DO(NI,NJ)+Z*Z*D1(NI,NJ)+X*Z*Z*C2(NI,NJ)
        +X*X*X*Z*D1(NI,NJ)+X*Z*Z*C2(NI,NJ)

1
300 CONTINUE
C(5,5)=GSTAR0*A*GSTARL*Z*
ADD1=-XMUL*(P+DEL_P*Y/L)*SNBT
ADD2= XMUL*(P+DEL_P*Y/L)*CSBT
FP(1)=FP(1)+ADD1
FP(2)=FP(2)+Y*ADD1
FP(3)=FP(3)+ADD2
FP(4)=FP(4)+Y*ADD2
FP(5)=FP(5)+Y *ADD2* Y
FP(6)=FP(6)+Y *ADD2* Y* Y
FP(7)=C.
FP(8)=C.
DO 400 CC 11=1,5
DO 400 CC  JJ=1,E
DO(11,JJ)=C.
DO 400 MM=1,5
DO 400 DD(11,JJ)=DD(11,JJ)+C(11,MM)*PHI(MM,JJ)
DO 400 CC 11=1,E
DO 400 CC  JJ=1,E
DO 400 MM=1,5
430 G(11,JJ)=G(11,JJ)+PHI(MM,11)*DD(MM,JJ)*X*ML
450 CONTINUE
CSBT2=CSBT*CSBT
CSBT4=CSBT*CSBT*2
DO 1CCC 11=1,E
DO 1CCC JJ=1,E
1000 PHIP1(11,JJ)=C.
PHIP1(2,2)=SNBT*SNBT*CSBT12
PHIP1(2,4)=-SNBT*CSBT12*CSBT
PHIP1(2,5)=-2.*SNBT*Y*CSBT12*CSBT
PHIP1(2,6)=-3.*SNBT*Y*Y*CSBT12*CSBT
PHIP1(4,2)=PHIP1(2,4)
PHIP1(4,4)=CSBT4
PHIP1(4,5)=2.*Y*CSBT4
PHIP1(4,6)=2.*Y*Y*CSBT4
PHIP1(5,2)=PHIP1(2,5)
PHIP1(5,4)=PHIP1(4,5)
PHIP1(5,5)=4.*Y*Y*CSBT4

```

BEST AVAILABLE COPY

```

PHIPI(5, E) = E.*Y**3*C SB T4
PHIPI(6, 2) = PHIPI(2, E)
PHIPI(6, 4) = PHIPI(4, E)
PHIPI(6, 5) = PHIPI(5, E)
PHIPI(6, 6) = S.*Y**4*C SB T4
DO 11CC II=1,E
DO 11CC JJ=1,E
PHIPA(II,JJ)=C.
DO 11CC MM=1,E
1100 PHIPI(II,JJ)=PHIPA(II,JJ)+PHIPI(II,MM)*AA(MM,JJ)*XMUL
CONTINUE
DO 55C II=1,E
DO 55C MM=1,E
500 FPA(II)=FPA(II)+AA(MM,II)*FP(MM)*2.*FI
WRITE(11,FPA(1),FPA(2),FPA(3),FPA(5),FPA(6),FPA(7))
1.CSPHI,CSPHJ,SNPHI,SNPHJ
DO 55C II=1,E
550 FK1+II)=FK1+II)+FPA(II)
DO 6 N1=1,E
DO 6 N2=1,E
DO 6 N3=1,E
6 GAA(N1,N2)=GAA(N1,N2)+G(N1,N3)*AA(N3,N2)
DO 7 N1=1,E
DO 7 N2=1,E
S(N1,N2)=C.
DO 7 N2=1,E
7 S(N1,N2)=S(N1,N2)+AA(N3,N1)*GAA(N3,N2)
DO 12CC II=1,E
DO 12CC JJ=1,E
SI(II,JJ)=C.
DO 12CC MM=1,E
1200 SI(II,JJ)=SI(II,JJ)+AA(MM,II)*PHIPA(MM,JJ)
DO 12CC II=1,E
DO 12CC JJ=1,E
1300 SI(II,JJ)=SI(II,JJ)+SI(II,JJ)*FNJ
DO 8 N1=1,E
DO 8 N2=1,E
8 S(N1,N2)=S(N1,N2)*2.*PI
RETURN
END

```

BEST AVAILABLE COPY

```

SUBROUTINE AMAT(AA,SNPSI,CSPSI,L,SNBTI,CSBTI,SBETJ,CSBTJ)
REAL L
DIMENSION AA(8,8)
TNBTI=SNBTI/C SBTI
TNBTJ=SNBTJ/C SBTJ
A1=TNBTI/L
A2=(2.*TNBTI+TNBTJ)/L/L
A3=(TNBTI+TNBTJ)/L/L/L
B1=1./C SBTI/C SBTI
B2=B1/L
B3=B2/L
B4=1./C SBTJ/C SBTJ/L
B5=B4/L
DO 10 N1=1,6
DO 10 N2=1,6
10 AA(N1,N2)=C.
AA(1,1)= SNPSI
AA(1,2)=-CSPSI
AA(2,1)=-SNPSI/L
AA(2,2)= CSPSI/L
AA(2,5)=-AA(2,1)
AA(2,6)=-AA(2,2)
AA(3,1)=-AA(1,2)
AA(3,2)=AA(1,1)
AA(4,1)=-Ai*SNPSI
AA(4,2)=A1*CSPSI
AA(4,3)=B1
AA(4,5)=-AA(4,1)
AA(4,6)=-AA(4,2)
AA(5,1)=A2*SNPSI-3.*CSPSI/L/L
AA(5,2)=-A2*CSPSI-3.*SNPSI/L/L
AA(5,3)=-2.*B2
AA(5,5)=-AA(5,1)
AA(5,6)=-AA(5,2)
AA(5,7)=-B4
AA(6,1)=-A3*SNPSI+2.*CSPSI/L/L/L
AA(6,2)=A3+CSPSI+2.*SNPSI/L/L/L
AA(6,3)=B3
AA(6,5)=-AA(6,1)
AA(6,6)=-AA(6,2)

```

BEST AVAILABLE COPY

```

AA(6,7)=B5
AA(7,4)= 1.
AA(8,4)=-1./L
AA(8,6)= 1./L
RETURN
END
SUBROUTINE PHIMAI(PHI,CSPBT,SNBT,SNPSI,CSPSI,RR,KAPPAL,Y,CSPHIX)
REAL KAPPAL
DIMENSION PHI(5,E)
DO 10 N1=1,5
DO 10 N2=1,E
  PHI(N1,N2)=C.
  PHI(1,2)= CSBT*CSPHIX
  PHI(1,4)= SNBT*CSPHIX
  PHI(1,5)= PHI(1,4)*2.*Y
  PHI(1,6)= PHI(1,4)*3.*Y*Y
  PHI(2,1)= SNPSI/RR
  PHI(2,2)= PHI(2,1)*Y
  PHI(2,3)= CSPSI/RR
  PHI(2,4)= PHI(2,3)*Y
  PHI(2,5)= PHI(2,4)*Y
  PHI(2,6)= PHI(2,5)*Y
  PHI(3,2)= (SNBT*SNB1-CSBT*CSPHIX) *KAFFAI
  PHI(3,4)=-2.*CSBT*SNBT *KAPPAL
  PHI(3,5)=-4.*CSBT*SNBT*Y *KAPPAL-2.*CSBT**3
  PHI(3,6)=-6.*CSBT*SNE1*Y*Y *KAPPAL-6.*Y*CSBT**3
  PHI(3,E)=-CSBT
  PHI(4,2)=-SNB1*CSPHIX/RR
  PHI(4,4)=-CSPHIX/RR*CSBT*LSBT
  PHI(4,5)=-CSPHIX/RR*2.*Y*CSBT*CSBT
  PHI(4,6)=-CSPHIX/RR*3.*Y*Y*CSBT*CSBT
  PHI(4,7)=-CSPHIX/RR
  PHI(4,8)=-CSPHIX/RR*Y
  PHI(5,7)=-1.
  PHI(5,E)=-Y
RETURN
END
SUBROUTINE STRSTFL(KI,RJ,TI,TJ)
REAL L,KAPPAL,KAPPAJ
COMMON ISF11 (23CC)

```

BEST AVAILABLE COPY

```

COMMON CSPHI,SNBTJ,CSPHI,CSBTJ,SNBTJ
1  * SNBTJ,SNBTJ,CSBTJ,CSBTJ
COMMON S(8,8),GE(8),AA(8,8),G(8,8),GAA(8,8)
1+LL1(1CCC),R(250),Z(25C),U(1000,8),F(1000)
2,J(25C),K(25C),ALP(250),PHAI(250),KAPP(250)
3,IPP(25C),C(5,5),SS(10,8),SE(10,8)
4,MAYER(25C),P(25C),TT(250)
5,LID(25C),DP(1CCC)
COMMON /SE T3/AU(2,2),AL(2,2)*DSTAR(2,2)*DISTAR(2,2),
1DSTAR(2,2),DC(2,2),DL(2,2),DI(2,2),L2(2,2),GBAR,GBARL
DIMENSION PHI(5,E),PHIA(5,8)
GSTAR=TI/GBARL
GSTARL=1J/GBARL
DO 25C NI=1,5
DO 25C NJ=1,5
250 C(NI,NJ)=C.
CALL PHIMAT(PHI,CSBTJ,SNBTJ,SNPSI,CSPHI,RI,KAPPAJ,0.,CSPHI)
DO 3C NJ=1,5
DO 3C N2=1,E
PHIA(N1,N2)=C.
DO 3C N3=1,E
30 PHIA(N1,N2)=PHIA(N1,N2)+PHI(N1,N3)*AA(N3,N2)
DO 3CC NI=1,2
DO 3CC NJ=1,2
C(NI,NJ)=AU(NI,NJ)
C(NI,NJ+2)=USTARC(NI,NJ)
C(NI+2,NJ)=C(NI,NJ+2)
300 C(NI+2,NJ+2)=DC(NI,NJ)
C(5,5)=GSTARO
DO 4C NI=1,E
DO 4C N2=1,E
SE(N1,N2)=PHIA(N1,N2)
SS(N1,N2)=C.
DO 4C N3=1,E
40 SS(N1,N2)=SS(N1,N2)+C(N1,N3)*PHIA(N3,N2)
CALL PHIMAT(PHI,CSBTJ,SNBTJ,SNPSI,CSPHI,RI,KAPPAJ,L,CSPHI)
DO 45 NI=1,5
DO 45 NJ=1,5
PHIA(N1,N2)=C.
DO 45 N3=1,E

```

BEST AVAILABLE COPY

```

ORTHOB2
ORTHOB3
ORTHOB4
ORTHOB5
ORTHOB6
ORTHOB7
ORTHOB8
ORTHOB9
ORTHOB10
ORTHOB11
ORTHOB12
ORTHOB13
ORTHOB14
ORTHOB15
ORTHOB16
ORTHOB17
ORTHOB18
ORTHOB19
ORTHOB20
ORTHOB21
ORTHOB22
ORTHOB23
ORTHOB24
ORTHOB25
ORTHOB26
ORTHOB27
ORTHOB28
ORTHOB29
ORTHOB30
ORTHOB31
ORTHOB32
ORTHOB33
ORTHOB34
ORTHOB35
ORTHOB36
ORTHOB37
ORTHOB38
ORTHOB39
ORTHOB40
ORTHOB41

```

```

45 PHIA(N1,N2)=PHIA(N1,N2)+PHI1(N1,N3)*AA(N3,N2)
      DO 460 N1=1,2
      DO 460 NJ=1,2
      C1(N1,NJ)=AL(N1,NJ)
      C1(N1,NJ+2)=USTARL(N1,NJ)
      C1(N1+2,NJ)=C(N1,NJ+2)
      400 C1(N1+2,NJ+2)=DC(N1,NJ)
      C1(5,5)=GSTARL
      DO 50 N1=1,5
      DO 50 NJ=1,5
      SE(N1+5,N2)=PHIA(N1,N2)
      SS(N1+5,N2)=C.
      DO 50 N3=1,5
      50 SS(N1+5,N2)=SS(N1+5,N2)+C(N1,N3)*PHIA(N3,N2)
      200 RETURN
      END

      SUBROUTINE STRESS(M,INCR,NINCR)
      REAL KAPP
      REAL NULC,NULCL
      COMMON EL(1C),EC(10),NULC(10),NULCL(10),GL(10)
      *,FSAVE(1CCC),XK(25C),F1(10C0)
      COMMON ISFC(12)
      COMMON S(E,E),GE(8),AA(8,8),G(8,8),GA(8,8)
      1,LL1(1CCC),R(25C),Z(25C),L1(1000,8)*F(1000,
      2,J(250),K(25C)*AL(250),PHA(250),KAPP(250)
      3,IPPI(25C),C(5,5),SS(10,8)*SE(10,8)
      4,MLAYER(25C),PP(25C),TT(25C)
      5,LID(25C),UP(1CCC)
      DIMENSION EPS(4),SIG(4),TAU13(2),GAMMA(2),CC(2,2)
      DIMENSION FD(1C)
      DIMENSION FE(E),FF(10)
      FINCR=INCR
      FNINCR=NINCR
      FAC1=FINCR/FNINCR
      PI=3.141592654
      REWIND 1
      IF(INCR.EQ.NINCR)REWIND 2
      IF(INCR.EQ.NINCR)REWIND 3
      IF(INCR.EQ.NINCR)WRITE(6,570)
      570 FORMAT(1H1,5CX,*LTPLT DATA*,//)

```

BEST AVAILABLE COPY

```

*   EX,*LL. NC.*.3X,*1/J*,2X,*COORDINATES*.25X.*FORCE* RESUORTOEE2
*   SULTANTS*.25X.*MCMENIT RESULTANTS* ORTHO883
*   /21X.*R*.7X.*Z*,9X,*LCAG. RESULT*,5X,*CIRC. RESULT.*,4X,*ORTHO884
*   SHEAR RESULT.*,EX,*LCAG. MCMENIT*,5X,*CIRC. MCMENIT*) ORTHO885
DU 7EC 11=1,M ORTHO886
111 ORTHO887
K1=4*(J(1)-1) ORTHO888
K2=4*(K(1)-1) ORTHO889
DO 597 I2=1,E ORTHO890
C E,7 GE(12)=C. ORTHO891
DU E1C JJ=1,4 ORTHO892
C IF(LL1(K1+JJ)*EQ.1)GC TC 6C6 ORTHO893
GE(JJ)= F(K1+JJ) ORTHO894
C 606 IF(LL1(K2+JJ)*EQ.1)GC TC 610 ORTHO895
GE(JJ+4)= F(K2+JJ) ORTHO896
610 CONTINUE ORTHO897
READ (1) FRJ,FZJ,FMJ,FRK,FZK,FMK,CSPHI,SNPHI,SNPHJ READ (1)I,S,SS,RJ,KJ,T,SE ORTHO898
DO 612 N1=1,E ORTHO899
FE(N1)=C. ORTHO9C0
DO 611 N2=1,E ORTHO9C1
611 FE(N1)*FE(N1)+SIN1*N2)*CE(N2) ORTHO9C2
IF((N1).GT.C.AND.(N1.LT.5)FE(N1)=FE(N1)/2./PI/R1 ORTHO9C3
IF((N1.GT.4.AND.N1.LT.9)FE(N1)=FE(N1)/2./PI/RJ ORTHO9C4
612 CONTINUE ORTHO9C5
DE1=2.*PI*R1/FAC1 ORTHO9C6
DEJ=2.*PI*RJ/FAC1 ORTHO9C7
FRJ=FRJ/DE1 ORTHO9C8
FZJ=FZJ/DE1 ORTHO9C9
FMJ=FMJ/DE1 ORTHO910
FRK=FRK/DEJ ORTHO911
FZK=FZK/DEJ ORTHO912
FMK=FMK/DEJ ORTHO913
UC=GE(1)*CSPHI-GE(2)*SNPHI ORTHO914
WC=GE(1)*SNPHI+GE(2)*CSPHI ORTHO915
IF(I.LT.M) GU TO 4CC ORTHO916
UCK=GE(5)*CSPHJ-GE(6)*SNPHJ ORTHO917
WCK=GE(5)*SNPHJ+GE(6)*CSPHJ ORTHO918
400 CONTINUE ORTHO919
FL1=(FE(1)-FRJ)*CSPHI-(FE(2)-FZJ)*SNPHI ORTHO920

```

BEST AVAILABLE COPY

```

FQ1=(FE(1)-FRJ)*SNPHI+(FE(2)-FZJ)*CSPHI
FL2=(FE(5)-FRK)*SPHJ-(FE(6)-F2K)*SNFHJ
FQ2=(FE(5)-FRK)*SPHJ+(FE(6)-F2K)*CSFHJ
FE(3)=FE(3)-FMJ
FE(7)=FE(7)-FMK
XK(1)=XK(1)+FL2
DU 615 N1=1,1C
FF(N1)=C.
DO 615 N2=1,8
E15 FF(N1)=FF(N1)+SS(N1,N2)*GE(N2)
IF(R(J(1)).EQ.C.C) GC TC 8C5
GO TO E1C
E05 FQ1 = C.C
FE(3) = FE(7)
FF(4) = FF(5)
FF(2) = FF(7)
FL1 = FL2
E10 CONTINUE
IF(INCR.NE.NINCR) GC TC 78C
WRITE(6,612),J(1),R(J(1)),Z(J(1)),F11,FF(2),FC1,FE(3),FF(4),
1K(1),R(K(1)),Z(K(1)),FL2,FF(7),F(2,FE(7),FF(9),
E13 FORMAT(1HC16,11C,CPIF8.3,1P5E18.7/117,0P2F8.3,1P5E18.7)
DO 617 N1=1,1C
FD(N1)=C.
DO 617 N2=1,8
E17 FD(N1)=FD(N1)+SE(N1,N2)*GE(N2)
N1AYER=MLAYER(1)
DO 8CC L1=1,NAYER
READ(3) MT,ANGLE,H1,HNI,HJ,HNJ,CC,T1,TJ
EPS(1)=FD(1)+FD(3)*(H1+HNI)/2.
EPS(2)=FD(2)+FD(4)*(H1+HNI)/2.
EPS(2)=FD(6)+FD(8)*(HJ+HNJ)/2.
EPS(4)=FD(7)+FD(9)*(HJ+HNJ)/2.
SIG(1)=CC(1,1)*EPS(1)+CC(1,2)*EPS(2)
SIG(2)=CC(2,1)*EPS(1)+CC(2,2)*EPS(2)
SIG(3)=CC(1,1)*EPS(3)+CC(1,2)*EPS(4)
SIG(4)=CC(2,1)*EPS(3)+CC(2,2)*EPS(4)
TAU12(1)=FQ1/T1
TAU13(2)=FC2/TJ
GAMMA(1)=TAU13(1)/GL(MT)

```

BEST AVAILABLE COPY

```

GAMMA(2)=TAU13(2)/GL(MT)
WRITE(2) 1 ,H1 ,HN1 ,L1 ,J(1) ,EPS(1) ,EPS(2) ,GAMMA(1) ,SIG(1) ,
1 ,TAU13(1) ,K(1) ,EPS(3) ,EPS(4) ,GAMMA(2) ,SIG(3) ,SIG(4) ,TAU13(2) ,
800 CONTINUE
780 CONTINUE
IF(INCR .NE. NINCR) GO TO 814
REWIND 2
WRITE(6,571)
571 FORMAT( //,5CX,*FIBER STRAINS AND STRESSES*/,
1IX,* ELEMENT*3*X*H1*5*X*HN1*3X*LAYER*2X*1/J*5X*EPS(1)*10X*EPS(2)*
21CX*GAMMA*1CX*SIG(1)*1C)*SIG(2)*10X*TAU13*)
DO 782 II=1,M
NAYER=MAYER(II)
DO 781 JJ=1,NAYER
READ(2) 1 ,HI ,HN1 ,L1 ,J(1) ,EPS(1) ,EPS(2) ,GAMMA(1) ,SIG(1) ,
1 ,TAU13(1) ,K(1) ,EPS(3) ,EPS(4) ,GAMMA(2) ,SIG(3) ,SIG(4) ,TAU13(2) ,
1 ,HI ,HN1 ,L1 ,J(1) ,EPS(1) ,EPS(2) ,GAMMA(1) ,SIG(1) ,SIG(2) ,ORTHO978
WRITE(6,E13) 1 ,HI ,HN1 ,L1 ,J(1) ,EPS(1) ,EPS(2) ,GAMMA(2) ,SIG(3) ,
1 ,TAU13(1) ,K(1) ,EPS(3) ,EPS(4) ,GAMMA(2) ,SIG(3) ,SIG(4) ,TAU13(2) ,
781 CONTINUE
782 CONTINUE
813 FORMAT(1HC16,2F8.3,215 ,1P6E16.7/133 ,1P6E16.7)
814 CONTINUE
814 RETURN
END
SUBROUTINE ELASMAT(MT,HI,HN1,ANGLE1,IJK,HJ,HNJ,TI,TJ)
REAL NLLC,NLLC
COMMON EL(1C),EC(10),NUCL(10),GL(10)
* ,FSAVE(1CCC),XK(25C),FI(1000)
COMMON ISFCM(144C1)
COMMON /SET3/AO(2,2),AL(2,2),DSTAR0(2,2),DSTAR1(2,2),
IDSTAR1(2,2),DO(2,2),DL(2,2),D1(2,2),D2(2,2),GBAR0,GBAR1
DIMENSION C(2,2)
ANGLE=ANGLE1*3.1415926/180.
DEMON=1.-NUCL(MT)*NUCL(MT)
C(1,1)=EL(MT)/EC(MT)
C(1,2)=NUCL(MT)*C(1,1)
C(2,1)=C(1,2)
C(2,2)=EC(MT)/EC(MT)
IF(ANGLE.EQ.C.) GO TO 615
CS=CUSIANGLE)

```

BEST AVAILABLE COPY

```

SN=SIN(ANGLE)
CS2=CS*CS
SN2=SN*SN
CS4=CS2*CS2
SN4=SN2*SN2
C11=CS4*C(1,1)+2.*SN2*CS2* C(1,2)+SN4*C(2,2)
C22=SN4*C(1,1)+2.*SN2*CS2* C(1,2)+CS4*C(2,2)
C12=SN2*CS2*(C(1,1)+C(2,2))+C(1,2)*(SN4+CS4)
C(1,1)=C11
C(1,2)=C12
C(2,1)=C(1,2)
C(2,2)=C22
615 CONTINUE
      WRITE(3) MT,ANGLE,HI,HNI,HJ,HNJ,C,TI,TJ
      DO 620 I=1,2
      DO 620 J=1,2
      AO(I,J)=AO(I,J)+C(I,J)*(HI-HNI)
      AL(I,J)=AL(I,J)+C(I,J)*(HJ-HNJ)
      DSTAR0(I,J)=DSTAR0(I,J)+C(5*C(I,J)*(HI*HI-HNI*HNI)
      DSTAR1(I,J)=DSTAR1(I,J)+0.5*C(I,J)*(HJ*HJ-HNJ*HNJ)
      DSTAR1(I,J)=DSTAR1(I,J)+C(I,J)*(HI*HJ-HNI*HNJ)
      DO(I,J)=DO(I,J)+C(I,J)*(HI*HI*HI-HNI*HNJ*HNJ)/3.
      DL(I,J)=DL(I,J)+C(I,J)*(HJ*HJ*HJ-HNJ*HNJ*HNJ)/3.
      D1(I,J)=D1(I,J)+C(I,J)*(HI*HI*HJ-HNI*HNJ)
      D2(I,J)=D2(I,J)+C(I,J)*(HI*HJ*HJ-HNI*HNJ*HNJ)
      GBAR0=GBAR0*(HI-HNI)/(TI*GL(WT))
      GBARL=GBARL*(HJ-HNJ)/(TJ*GL(WT))
      RETURN
      END
      ORTH10C2
      ORTH10C3
      ORTH10C4
      ORTH10C5
      ORTH10C6
      ORTH10C7
      ORTH1008
      ORTH10C9
      ORTH10C10
      ORTH1011
      ORTH1012
      ORTH10C13
      ORTH1014
      ORTH1015
      ORTH1016
      ORTH10C17
      ORTH1018
      ORTH1019
      ORTH10C20
      ORTH1021
      ORTH1022
      ORTH1023
      ORTH1024
      ORTH1025
      ORTH1026
      ORTH10C27
      ORTH1028
      ORTH1029
      ORTH10C30

```

BEST AVAILABLE COPY

REFERENCES

1. Zienkiewicz, O. C. and Holister, G. S. (editors), Stress Analysis: Recent Developments in Numerical and Experimental Methods, New York, John Wiley and Sons, 1965.
2. Zienkiewicz, O. C., The Finite Element Methods in Engineering Science, London, McGraw-Hill, 1971.
3. Przemieniecki, J. C., The Theory of Matrix Structural Analysis, New York, McGraw-Hill, 1968.
4. Desai, C. S. and Abel, J. F., Introduction to the Finite Element Method, New York, van Nostrand Reinhold, 1972.
5. Martin, H. C. and Carey, G. F., Introduction to Finite Element Analysis, New York, McGraw-Hill, 1973.
6. Meyer, R. R. and Harmon, M. B., "Conical Segment Method for Analyzing Open Crown Shells of Revolution for Edge Loadings," AIAA J., Vol. 1, No. 4, April 1963, pp. 886-891.
7. Popov, E. P., Penzien, J. and Lu, Z. A., "Finite Element Solution for Axisymmetric Shells," J. of EM Proc. ASCE, Vol. 90, No. EM5, October 1964, pp. 119-145.
8. Grafton, P. E. and Strome, D. R., "Analysis of Axisymmetrical Shells by the Direct Stiffness Method," AIAA J., Vol. 1, No. 10, October 1963, pp. 2342-2347.
9. Jones, R. E. and Strome, D. R., "Direct Stiffness Method Analysis of Shells of Revolution Utilizing Curved Elements," AIAA J., Vol. 4, No. 9, September 1966, pp. 1519-1525.
10. Khojasteh-Bakht, J., "Analysis of Elastic-Plastic Shells of Revolution Under Axisymmetric Loading by the Finite Element Method," Ph.D. Dissertation, Department of Civil Engineering, University of California, Berkeley, California.
11. Clough, R. W. and Felippa, C. A., "A Refined Quadrilateral Element for Analysis of Plate Bending," Proceedings Second Conference on Matrix Methods in Structural Mechanics, Wright-Patterson AFB, Ohio, 1968.
12. Klein, Stanley, Matrix Methods in Structural Mechanics, Report No. AFFDL-TR-66-80, Air Force Flight Dynamics Laboratory and Air Force Institute of Technology Air University, November 1966.

13. Sharifi, Parviz, "Nonlinear Analysis of Sandwich Structures," Ph.D. Dissertation, Department of Civil Engineering, University of California, Berkeley, California, 1970.
14. McNamara, John F., "Incremental Stiffness Method for Finite Element Analysis of the Nonlinear Dynamic Problem," Ph.D. Dissertation, Division of Engineering, Brown University, 1972.
15. Becker, Eric B., and Brisbane, John J., Application of the Finite Element Method to Stress Analysis of Solid Propellant Rocket Grains, Vol. 1, Rohm and Haas Company, Report No. S-76, November 1965.
16. Nickell, Robert E., and Sato, Tomio, Finite Element Stress Analysis of Orthotropic, Layered Shells of Revolution Using a Curved Shell Element, Rohm and Haas Company, Report No. S-264, October 1970.
17. Reissner, E., "On Bending of Elastic Plates," Quarterly Applied Mathematics, Vol. 5, No. 1, April 1947.
18. Novozhilov, V. V., Foundations of the Nonlinear Theory of Elasticity, New York, Graylock Press, 1953.
19. Tsao, C. H., "Strain-Displacement Relations in Large Displacement Theory of Shells," AIAA J., Vol. 2, No. 11, 1964, pp. 2060-2062.
20. Plantema, F. J., Sandwich Construction, John Wiley and Sons, New York, 1966.
21. Kraus, H., Thin Elastic Shells, New York, John Wiley and Sons, 1967.
22. Naghdi, P. M., "Foundations of Elastic Shell Theory," Progress in Solid Mechanics, I. N. Sneddon and R. Hill (editors), Amsterdam, North-Holland, 1963.
23. Timoshenko, S. and Woinowsky-Krieger, S., Theory of Plates and Shells, second edition, New York, McGraw-Hill, 1959.

DISTRIBUTION

	No. of Copies
Basic Distribution List	34
Defense Documentation Center Cameron Station Alexandria, VA 22314	12
Commander US Army Materiel Research and Development Command ATTN: DRCCG DRCRD 5001 Eisenhower Avenue Alexandria, VA 22333	1 1
DRCPM-RSE, Dr. Eldridge	20
DRSMI-LP, Mr. Voigt	1
DRDMI-T, Dr. Kobler -TL, Mr. Lewis -TLA, Mr. Pettey -TBD -TI (Reference Copy) (Record Copy)	1 1 1 3 1 1